GA–A26639

FUSION NUCLEAR SCIENCE FACILITY CANDIDATES

by
R.D. STAMBAUGH, V.S. CHAN, A.M. GAROFALO, M. SAWAN,
D.A. HUMPHREYS, L.L. LAO, J.A. LEUER, T.W. PETRIE,
R. PRATER, P.B. SNYDER, J.P. SMITH and C.P.C. WONG

JUNE 2010

GENERAL ATOMICS

DISCLAIMER

GA–A26639

FUSION NUCLEAR SCIENCE FACILITY CANDIDATES

by
R.D. STAMBAUGH, V.S. CHAN, A.M. GAROFALO, M. SAWAN,*
D.A. HUMPHREYS, L.L. LAO, J.A. LEUER, T.W. PETRIE,
R. PRATER, P.B. SNYDER, J.P. SMITH and C.P.C. WONG

This is a preprint of a paper to be to be submitted for publication in Fusion Science and Technology.

*University of Wisconsin-Madison, Wisconsin, USA

Work supported in part by
General Atomics Internal Funding and
by the U.S. Department of Energy
under DE-FG02-09ER54513

GENERAL ATOMICS PROJECT 40010
JUNE 2010

ABSTRACT

To move to a fusion DEMO power plant after ITER, a Fusion Nuclear Science Facility (FNSF) is needed in addition to ITER and research in operating tokamaks and those under construction. A Fusion Nuclear Science Facility will enable research on how to utilize and deal with the products of fusion reactions, such issues as how to extract the energy from the neutrons and the alpha particles into high temperature process heat streams to be either used directly or converted to electricity, how to make tritium from the neutrons and lithium, how to deal with the effects of the neutrons on the blanket structures, and how to manage the first wall surface erosion caused by the alpha particle heat appearing as low energy plasma fluxes to those surfaces. Two candidates for the FNSF are considered in this paper: normal- and low-aspect ratio copper magnet tokamaks. The methods of selecting optimum machine design points versus aspect ratio are fully presented. The two options are compared and contrasted; both options appear viable.

I. INTRODUCTION

The question has been raised [1] what else besides ITER [2] do we need to do to be able to move to a Demonstration fusion power plant (DEMO) after ITER? Reference [1] provides their working definition of DEMO and a discussion of varying international views of DEMO. For the last few years, we have suggested that a device we call the Fusion Development Facility [3–5] is the missing element needed to make possible a fusion demonstration power plant (DEMO) of the ARIES-AT type [6] as the next step after ITER. Characteristics of FDF should be [7] neutron flux at the outboard midplane of 1–2 MW/m^2, continuous operation for periods up to two weeks, a goal of a duty factor of 0.3 on a year and fluences of 3–6 MW-yr/m^2 in 10 years of operation to enable development of blankets suitable for tritium, electricity, and hydrogen production. Devices of this type have come to be known as Fusion Nuclear Science Facilities (FNSF) and viewed as the leading element of a Fusion Nuclear Science Program. Currently, a second candidate for the FNSF is the Spherical Tokamak-Component Test Facility (ST-CTF) [8,9]. The design, construction, and research done on an FNSF will motivate and be a part of a national Fusion Nuclear Science Program (FNSP), headed by FNSF and supported by seven major lines of research: high performance plasmas, plasma-material interactions, power extraction and fuel production, tritium processing, fusion materials, nuclear science computation, and measurements in the nuclear environment. Work done in the FNSP would to a great extent be of generic value to MFE, IFE, hybrids and also relevant to long burn fission systems.

Our purpose in this paper is to document fully and in detail the physics and engineering calculations we use to select and define optimum machines for the FNSF purpose so that other researchers can examine in detail and for themselves the basis for the machines suggested, or perhaps utilize material in this paper to devise their own suggestions. A second purpose is to document in detail two candidate types of machines aimed at the same FNSF scope. They are both copper coil tokamaks, the FDF at normal aspect ratio and the ST-CTF at very low aspect ratio. These machines would be essentially research devices, enabling fusion blanket research and development. The copper TF coils will have joints as in DIII-D, Alcator C-mod, and NSTX. The jointed TF coil allows a simple vertical maintenance scheme (see Section IV) which enables rapid changeout of the entire blanket and divertor, an effective maintenance scheme, and the kind of flexibility needed in a research device.

FDF and ST-CTF have many purposes in common. Briefly summarizing, FDF is intended to enable *development of fusion's energy applications and the operating modes needed in DEMO*. FDF should be used to *learn how to close the fusion fuel cycle and make electricity and hydrogen from the fusion process*. We believe that before a DEMO project can be committed, net *tritium production must be demonstrated and assured*. It is not practical to first make this demonstration in the initial phase of DEMO operation, owing to the high tritium consumption rates. Assurance of tritium self-sufficiency must be made first

in a more modest device. FDF will have a goal of producing its own tritium and building a supply to start up DEMO. The size of FDF (R = 2.7 m) and the significant level of fusion power produced (290 MW) require that FDF be self-sufficient in tritium. The approach taken will be to engineer a first full blanket with the primary goal of just producing net tritium. In parallel, more advanced blankets will be tested in port blanket modules and successful ones will then be engineered into second and third generation full blankets. FDF will be designed to facilitate changeout of the full first wall/blanket structures and will do so at least twice in the life of the project. The ST-CTF with only an outer blanket and without breeding in the divertor may not be able to achieve TBR greater than one. The ST-CTF's small size (R = 1.3 m) and lower fusion power (110 MW) mean the provision of 20% of its tritium (about 0.2 kg per year) from external supply may be feasible. It may be concluded that if the designed TBR (say 0.8) is achieved in ST-CTF, then the extension to DEMO merely involves covering more area with blankets of known local TBR performance. The ST-CTF concept should look hard at whether TBR > 1 can be achieved in that concept. These matters need resolution in the selection of concept; we continue to believe actually demonstrating net tritium production is an important next step milestone for fusion.

In port blanket modules, *the development of blankets suitable for both tritium production and electricity production will be made*. Both FDF and ST-CTF will provide the necessary facility to test perhaps ten different blanket concepts or variants in 2–3 ports over a 10 year time period. They share in common providing the necessary facility to learn how to make blankets that support high temperature and high thermodynamic efficiency for power conversion for electric power production. Another port site should be devoted to *the development of blankets that can support hydrogen production*, which can require even more demanding temperatures of extracted coolant, over 900°C. Although neither FDF nor ST-CTF intend to attempt electric power production from its full blankets, actual demonstrations of both electricity production (100–300 kW) and of hydrogen production (one metric ton per week) should be made on the most successful port blankets.

With neutron flux at the outer midplane of 1–2 MW/m^2 and a goal of a duty factor on a year of 0.3, FDF and ST-CTF can *produce fluences of 3–6 MW-yr/m^2* in 10 years of operation onto complete blanket structures and/or material sample volumes of about 1 m^3. They can enable irradiation qualification of materials in port material sample exposure stations. This level of fluence should enable qualification of at least the first few years of DEMO operation.

FDF intends to *demonstrate advanced physics operation of a tokamak in steady-state with burn*. FDF will be designed using already proven and conservative implementations of all elements of Advanced Tokamak physics to produce 150–300 MW fusion power with modest energy gain (Q < 7) in a modest sized device. Modest size is needed to minimize the cost consistent with the mission. Even so, the cost will be substantial and the ambition of the mission must match the cost. Modest size means modest Q; in tokamaks size and Q are

strongly coupled. FDF with $Q < 7$ does is complementary to ITER in regards to high energy gain burning plasma research. Conservative AT physics will enable *full non-inductive, high bootstrap operation to demonstrate continuous operation of a tokamak for periods up to two weeks*, a necessary step before DEMO and essential to blanket development research. The ST-CTF shares the same ambitions in regard to steady-state operation, but intends to achieve that with very conventional physics operating modes as essentially a driven machine with the majority of the plasma current driven by auxiliary power.

Building on secure baseline operating modes, FDF must be capable of *further developing all elements of AT physics, qualifying them for an advanced performance DEMO*. The many advances made in the last decade must be captured in a next step device in order to make progress toward the even more advanced operating modes called for by ARIES-AT. The FDF, operating in a compact D-T regime prototypical of high power density fusion reactors, will provide burning plasma physics understanding to complement the contributions from the new Asian superconducting tokamaks and ITER (Fig. 1). The extent to which the ST-CTF may enable Advanced Tokamak physics toward DEMO is also examined in this paper.

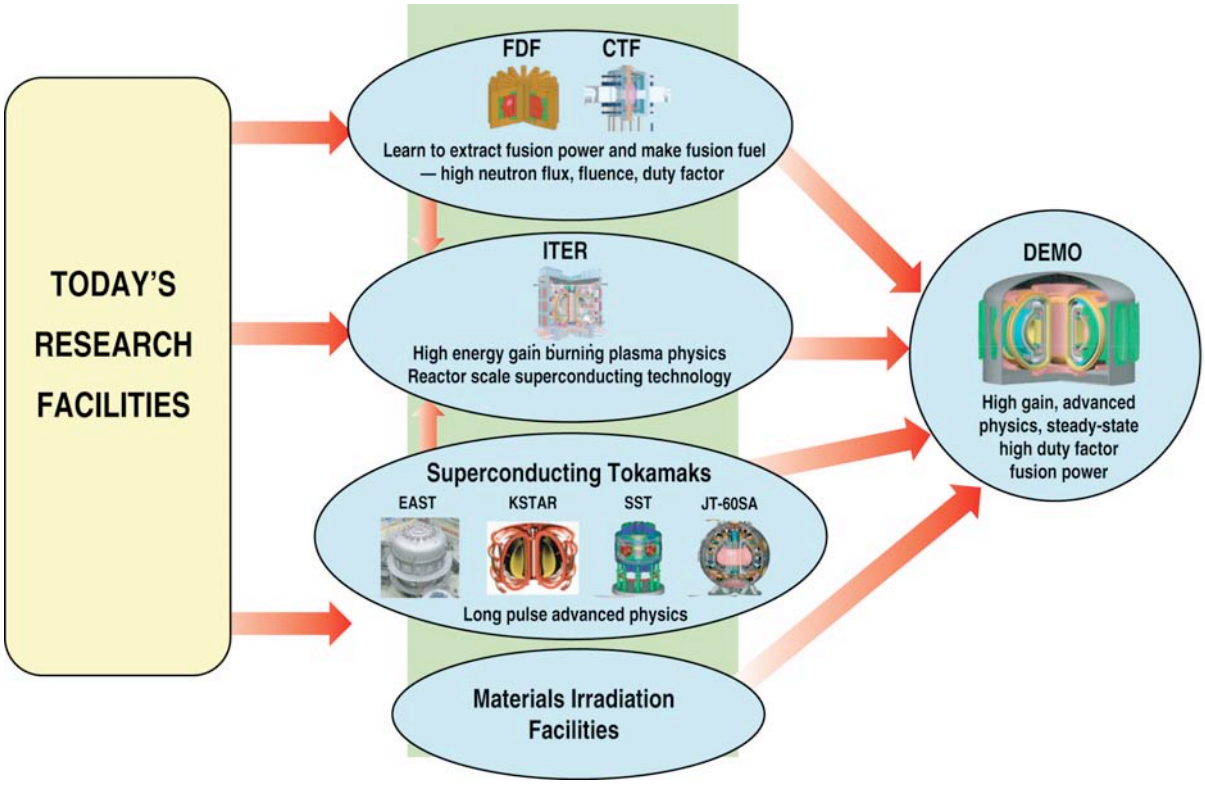

Fig. 1. A Fusion Nuclear Science Facility, ITER, Superconducting Tokamaks, and Materials Test Facilities enable DEMO.

II. THE BASIC MACHINE DESIGN SPREADSHEET

To evaluate tokamak fusion reactors or burning plasma development machines like FDF, an EXCEL spreadsheet was constructed that incorporates to the extent possible in 0-D the relevant physics constraints and engineering constraints. The spreadsheet can treat either copper or superconducting machines. The content of the basic spreadsheet is given in this section. In Section II.J we describe how the non-linear optimizer in EXCEL is used to drive the basic spreadsheet to create a range of optimized machine designs over aspect ratio. The cross section of our baseline FDF machine is shown in Fig. 2.

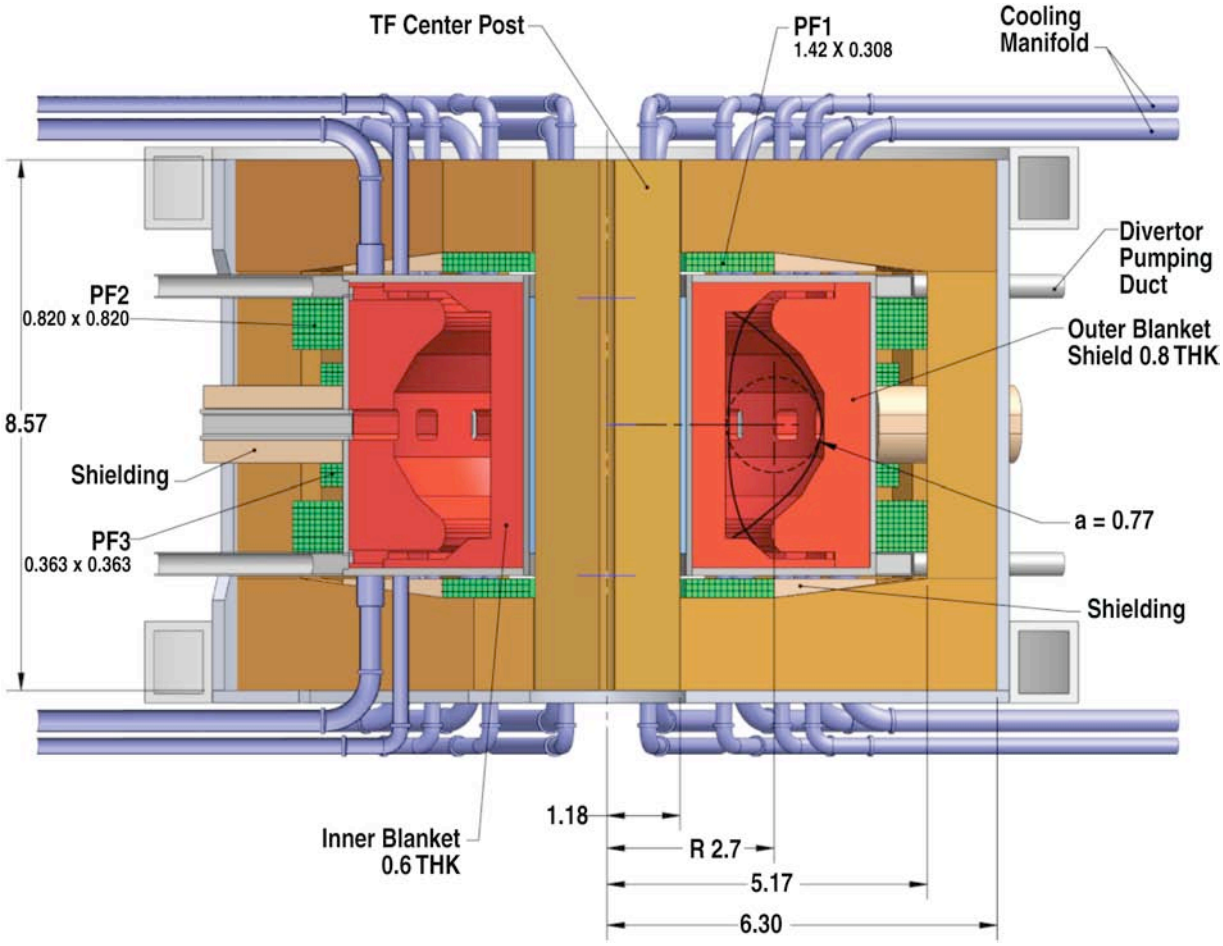

Fig. 2. Rebaselined FDF incorporating increased blanket/shield, realistic divertor geometry, plasma wall gaps.

II.A. BASIC MACHINE GEOMETRY

For each machine case, the aspect ratio A and the thickness of the inboard blanket/shield δB_{in} and outboard blanket/shield δB_{out} are specified. These blanket/shield thicknesses are chosen informed by the neutronics calculations described in Section III.A.10.

Other specified quantities are:

δRS — (radial build of the ohmic heating solenoid)

δRTF — (radial build of TF coil centerpost)

J_c — current density in centerpost

λ_c — fraction of the TF that is copper, generally taken as 0.9

λ_E — fraction of solenoid that is copper, generally taken as 0.75

η_c — resistivity of copper, generally taken as 0.02 micro-Ohm-meters

δ – plasma triangularity, generally taken as 0.7

δR_{in} – inner gap between the plasma and the first wall

δR_{out} – outer gap between the plasma and the first wall

Values for these gaps come from recommendations from DIII-D operating experience. The recommended inner gap is 7 times the midplane heat flux fall off length λ_q from Loarte et al. [10]. The recommended outer gap is 11 λ_q. Fixed values typical for a given machine class are often used, e.g., δR_{in} = 5 cm and δR_{out} = 8 cm.

The elongation $\kappa(A)$ is taken as a fraction, typically 95%, of the maximum stable elongation as a function of aspect ratio calculated in Ref. [11].

$$\kappa_{MAX} = 2.4 + 65\, e^{-A/(0.376)} \quad . \tag{1}$$

Provided suitable control coils and power supplies are provided, it was shown in Ref. [12] that a tokamak can operate stably within a few percent of the ideal limit to elongation.

In what follows, the units used are generally m, T, MW, MA, MA/m^2, MPa, kg, keV, and densities in units 10^{20} m^{-3}.

The radius of the TF coil centerpost centerline R_{TF} is specified. Generally it is taken as half the radial build of the TF coil so the TF coil is considered solid from the axis of symmetry of the machine, although options exist for a finite hole in the center and for the OH solenoid to be in that center hole. Such options are used for superconducting machines. The inner radius of the plasma is calculated as the sum of the outer radius of the TF coil plus the radial build of the solenoid, the blanket, and the inner gap. The vacuum vessel is considered part of the blanket. Then the minor radius of the plasma (a) is calculated as the inner radius of the plasma divided by ($A-1$) and the plasma major radius R_0 is then aA.

The plasma volume is then $V_P = 2\pi^2 R_0 a^2 \kappa(1 - 0.151\delta/A)$.

II.B. TOROIDAL COIL SECTION

After the physics calculations described below, the toroidal coil centerpost current density is generally adjusted to give a desired peak neutron wall loading at the outer midplane. The total current in the TF centerpost is $I_c = J_c * 2\pi R_{TF}\,\delta R_{TF}$. The toroidal field at the centerpost surface is $B_c = 0.2 * I_c / R_{TFOUTER}$. The toroidal field B_0 at the center of the plasma is $0.2 * I_c / R_0$.

The peak Von Meis stress in the centerpost is

$$S_{VM}(Pa) = \left(S_h^2 + S_{ax}^2 - S_h S_{ax}\right)^{1/2} \quad , \tag{2}$$

$$S_{VMK}(KSI) = 1.45 \times 10^{-7}\, S_{VM} \quad . \tag{3}$$

The average hoop stress in the TF coil is

$$S_{hPAV} = \frac{-\frac{2}{3}\left(R_0 B_0\right)^2 \left(2R_{TFIN} + R_{TFOUT}\right)}{\left(4\pi \times 10^{-7}\right)\left(R_{TFOUT} - R_{TFIN}\right)\left(R_{TFOUT} + R_{TFIN}\right)^2} \quad . \tag{4}$$

The peak hoop stress at the inside radius with voids is $S_h = S_{hPAV} * S_{PF} / \lambda$

$$S_{PF} = 2; \text{ peaking factor} \quad . \tag{5}$$

The average axial stress on the centerpost leg is

$$S_{axav} = 0.5 \ln\left[\frac{\left(R_{ROUT} + R_{RIN}\right)}{2\left(\frac{R_{TFOUT}^2 + R_{TFIN}^2}{2}\right)^{1/2}}\right] \frac{\left(R_0 B_0\right)^2}{4\pi \times 10^{-7}\left(R_{TFOUT}^2 - R_{TFIN}^2\right)} \quad , \tag{6}$$

and the peak axial stress with voids is $S_{ax} = S_{axav} / \lambda_c$. Upper limits on these stresses are used as constraints in machine designs.

The steady state temperature rise in the centerpost is

$$\Delta T_{CW}(^\circ K) = \frac{P_c}{4.186\, A_c\, (1-\lambda)\, v_w} \quad , \tag{7}$$

assuming a water flow velocity of 10 m/s in a one pass, straight through path. An upper limit on this temperature rise is used as a constraint.

The toroidal coil is considered to be rectangular coil made up of the cylindrical centerpost connected top and bottom to straight vertical return legs by radial wedge sections.

An allowance for divertor space above the X-points is made.

$$\delta_{DIV} = 0.25a \quad . \tag{8}$$

The blanket thickness in the divertor areas is taken as 83% of the inner blanket thickness based on the neutronics calculations. The total height of the TF centerpost is then

$$H_{BORE} = 2a\kappa + 2\left(\delta_{DIV} + 0.83\,\delta B + h_w + \delta Z_{PF1}\right) \quad , \tag{9}$$

where h_w is the height of the radial wedge section and δZ_{PF1} is the vertical height of the divertor PF coil (see below).

Then the resistance of the centerpost is

$$R_{CP} = \frac{\eta H_{BORE}}{\lambda_c A_C} \quad , \tag{10}$$

where A_c is the area of the centerpost.

The power dissipated in the centerpost is then

$$P_C = I_C^2 R_{CP} \quad . \tag{11}$$

The vertical return legs are between an inner radius (R_{RIN}) just outside the PF coils and an outer radius (R_{ROUT}) given by the relations below. The return legs are considered to occupy half of the toroidal circumference at their radius. The radial thickness of the return legs is taken to correspond to a low, specified average current density (typically $J_{RTF} = 4$ MA/m^2) to minimize the resistive dissipation in the return legs.

$$C_{RTF} = 0.5\,(2\pi R_{RIN}) \quad , \tag{12}$$

$$\delta R_{RTF} = \frac{I_C}{J_{RTF}\, C_{RTF}};\ J_{RTF} = 4\ \text{MA/m}^2 \quad , \tag{13}$$

$$R_{RIN} = R_{PFO};\ R_{ROUT} = R_{PFO} + \delta R_{RTF} \quad , \tag{14}$$

The resistance of the return legs is then

$$R_{RTF} = \frac{\eta H_{BORE}}{\lambda C_{RTF} \delta R_{RTF}} \quad , \tag{15}$$

The radial sections that connect the TF centerpost to the TF return legs are in two parts. First, there is a wedge section of fixed vertical dimension extending above the divertor coil to the divertor coil's outer radius $R_{PF1\,OUT}$ from the outer radius of the centerpost $R_{TF\,OUTER}$.

The resistance of one (upper or lower) of these wedges is

$$R_{WIN} = \frac{\eta}{\lambda_c h_w} \ln\left(\frac{R_{PF1OUT}}{R_{TF\,OUTER}}\right) \quad , \tag{16}$$

Then the second, outer wedge connects from the above wedge to the TF return leg, tapering both radially and vertically to provide space for divertor pumping ducts. The height of this wedge at the TF return legs is $h_{w2} = h_w + \delta Z_{PF1}$

The resistance of one (upper or lower) of these wedges is

$$R_{WOUT} = \frac{\eta\left(0.5\,R_{RIN} - R_{PF1OUT}\right)}{2\lambda c\left[2\pi\left(R_{PF1OUT} + 0.5R_{RIN}\right)\left(h_{w2} - h_w\right)\right]} \times \ln\left(\frac{h_{w2}}{h_w}\right) \quad . \tag{17}$$

The total power dissipated in the wedges P_W is twice the TF current squared times ($R_{WIN} + R_{WOUT}$).

The total power dissipated in the TF coil is the sum of the centerpost power, the wedge section power, and the return leg power. The factor F_R = 87% is to reflect how the TF current "rounds the corner" at the joint between the vertical sections and the wedges instead of going out the top and bottom of the centerpost before turning sideways out the wedge sections.

$$P_{TF} = F_R P_C + P_W + F_R P_{RTF} \quad , \tag{18}$$

and is generally around 200 MW. The TF coil section volumes, masses, and weights are calculated in the obvious manner.

II.C. OHMIC HEATING SOLENOID SECTION

The ohmic heating solenoid is generally considered to be wound on the outer radius of the TF coil centerpost, although options exist to look at OH solenoids on the inner major radius side of the TF centerpost, especially for superconducting cases. The radial thickness of the OH coil is specified. The current density in the OH coil is a specified number but is generally adjusted so that the OH solenoid single swung can produce enough volt-seconds to ramp up the plasma current to its full value. Stresses in the coil are then calculated. The outer and inner solenoid radii are:

$$\begin{aligned} R_{SOLOUT} &= R_{TFC} + 0.5\delta R_{TF} + \delta R_{SOL} \\ R_{SOLIN} &= R_{TF\,OUT} \end{aligned} \quad . \tag{19}$$

First the OH flux required to ramp up the plasma current to full value is calculated.

The external inductance is

$$L_{EXT} = 0.4\pi R_0 \left[\ln\left(\frac{8R_0}{a\sqrt{\kappa}} \right) - 2 \right] \quad . \tag{20}$$

The internal inductance is

$$L_{INT} = 0.4\pi R_0 \, l_i / 2 , \qquad l_i = 0.5 \quad . \tag{21}$$

Then the plasma inductance is

$$L_P = L_{EXT} + L_{INT} \quad . \tag{22}$$

To estimate resistive volt-seconds, the standard Ejima coefficient $C_E = 0.4$ is used.

The ramp-up flux is estimated as

$$F_{RAMPUP} = \left(C_E \, 0.4\pi R_0 + L_P \right) I_P \quad . \tag{23}$$

An estimate must be made of the portion of this flux that will be supplied by the vertical field PF coils.

$$B_{VERT} = \frac{0.1 I_P}{R_0} \left[\ln\left(\frac{8R_0}{a\sqrt{\kappa}} \right) - 1.5 + \beta_P / 2 - \ell_i / 2 \right] \quad , \tag{24}$$

$$F_{VERT} = 0.8\pi B_{VERT} \left[R_0^2 - \left(R_0 - a \right)^2 \right] \quad . \tag{25}$$

Then the flux required from the OH solenoid is $F_{TOT} = F_{RAMPUP} - F_{VERT}$.

Next the flux actually produced by the OH solenoid is calculated.

The B field in the solenoid bore is

$$B_{SOL} = 0.4\pi J_{SOL} \left(R_{SOLOUT} - R_{SOLIN} \right) \quad . \tag{26}$$

The flux produced by the solenoid is

$$F_{SOL} = 0.4\pi J_{SOL} \frac{\pi}{3} \left(R_{SOLOUT}^3 - R_{SOLIN}^3 \right) \quad . \tag{27}$$

Then the ratio of the flux produced by the solenoid, half swung, to the flux needed to ramp up the plasma current to full value is calculated depending if the flux contributed by the other PF coils is included.

$$F_{RAMP} = F_{SOL} / F_{RAMPUP} \quad , \tag{28}$$

neglecting flux contribution from outer PF coils.

An alternative calculation, which is the one actually used, is

$$B_{SOLBORE} = 0.4\pi J_{SOL} R_{SOLOUT}\left(1-\frac{R_{SOLIN}}{R_{SOLOUT}}\right) \quad , \tag{29}$$

$$F_{SOL2} = \pi B_{SOLBORE} R_{SOLOUT}^2 \frac{\left[\left(\frac{R_{SOLOUT}}{R_{SOLIN}}\right)^2 + \frac{R_{SOLOUT}}{R_{SOLIN}} + 1\right]}{3} \quad , \tag{30}$$

$$F_{RAMP2} = F_{SOL2} / F_{TOT} \quad . \tag{31}$$

which includes the contribution from the outer PF coils.

The peak hoop stress in the solenoid is

$$S_{hSOL}\,(MPa) = 0.4\pi \frac{\left(J_{SOL}\, R_{SOLOUT}\right)^2}{12\lambda_{SOL}} * \left[\frac{3R_{oi}^3\left(\rho_p - 1\right) + R_{oi}^2\left(1-\rho_p\right) - R_{oi}\left(7\rho_p + 5\right) + 5\rho_p + 7}{1+R_{oi}}\right] \quad , \tag{32}$$

where ρ_p is Poisson's ratio (0.33) and $R_{oi} = R_{SOLOUT} / R_{SOLIN}$.

$$S_{hSOL}\,(KSI) = 0.145\, S_{hSOL}\,(MPa) \quad . \tag{33}$$

The average hoop stress in the solenoid is

$$S_{hSOLAV}\,(MPa) = \frac{0.4\,\pi J_{SOL}^2 R_{SOLOUT}^2}{6\lambda_{SOL}}\left(1 + R_{oi} - 2R_{oi}^2\right) \quad . \tag{34}$$

Next the rate of heating of the solenoid assuming it is only inertially cooled is calculated.

The volume and mass of the solenoid are

$$V_{SOL} = \pi(R_{SOLOUT}^2 - R_{SOLIN}^2)2a\kappa \quad , \tag{35}$$

$$M_{SOL} = 8960\, V_{SOL}\, \lambda_{SOL} \quad . \tag{36}$$

The total current and resistance of the solenoid are

$$I_{SOL} = J_{SOL}\, 2a\kappa (R_{SOLOUT} - R_{SOLIN}) \quad , \tag{37}$$

$$R_{SOL} = \eta_{SOL} \frac{2\pi(R_{SOLOUT} + R_{SOLIN})}{2[2a\kappa(R_{SOLOUT} - R_{SOLIN})]} \quad . \tag{38}$$

The power dissipated in the solenoid at full current is

$$P_{SOL} = I_{SOL}^2 R_{SOL} \quad . \tag{39}$$

The corresponding heating rate is

$$dT_{SOL}/dt = \frac{1000 P_{SOL}}{0.38 M_{SOL}} \quad . \tag{40}$$

Considering that the solenoid when half swung has a triangle shaped waveform for charging and discharging with a ramp time of δt_{RISE} and considering a maximum allowed temperature rise in the solenoid δT_{MAX}, the allowed rise time is calculated as

$$\Delta t_{RISE} = \frac{3\Delta T_{MAX}}{2 I_{SOL}^2 \left(\frac{1000 R_{SOL}}{0.38 M_{SOL}}\right)} \quad . \tag{41}$$

Then the corresponding rate of rise of the plasma current and the maximum loop voltage are

$$\dot{I}_P = \frac{I_P}{\Delta t_{RISE}} \quad , \tag{42}$$

$$V_{LOOPMAX} = F_{SOL2}/\Delta t_{RISE} \quad . \tag{43}$$

Both δt_{RISE} and the rate of rise of the plasma current and the maximum loop voltage are examined for reasonableness. Generally for an allowed 50 degree temperature rise, one finds the rise time allowed is about 4 s. The consideration of some degree of active cooling effect in the solenoid would increase that rise time.

II.D. POLOIDAL FIELD COILS

Three up-down symmetric pairs of PF coils are considered, only to calculate their resistive dissipation and include it in the overall power balance. Separate equilibrium calculations have informed what fractions of the plasma current these coils carry.

PF1 is the divertor coil and it is considered to carry 73% of the plasma current. The area is calculated by dividing the current in the coil by an assumed low current density (typically 11 MA/m^2) to minimize resistive dissipation. The radial extent of the coil is taken as the maximum of 0.5 m or the plasma minor radius plus the inner blanket thickness plus the inner gap. The height of the coil is then calculated from the area. The radius of the coil R_{1PF} is R_0 – half the radial extent of the coil. The resistance of the coil is then

$$R_{PF1} = \frac{\eta 2\pi R_{1PF}}{\lambda_{SOL} A_{PF1}} \quad . \tag{44}$$

The power is $P_{PF1} = I_{PF1}^2 R_{PF1}$. The volume is $V_{PF1} = 2\pi R_{1PF} A_{PF1}$. The mass is $M_{PF1} = 8960 V_{PF1}$.

PF2 is the upper outboard coil for vertical field. It is assumed to carry 51% of the plasma current. Its radius is the outer radius of the outer blanket. Its necessary area is calculated using an assumed current density typically 5 MA/m^2. It is considered a square coil with thickness the square root of the area. The resistance, power, volume, and mass calculations are the obvious calculations.

PF3 is the closest to the midplane outer PF coil. It is assumed to carry 12% of the plasma current. It is also assumed to have a current density typically 6 MA/m^2 and the necessary area then calculated. It is also assumed square with its thickness the square root of the area. Its radius is the outer radius of the outer blanket plus half its thickness. The resistance, power, volume, and mass calculations are the obvious calculations.

The total PF power is twice the sum of the power in the three PF coils, since the machine is up-down symmetric.

II.E. PLASMA PARAMETERS

The physics parameters are essentially all determined by the choice of aspect ratio using Ref. [11] for the maximum stable elongation as a function of aspect ratio and Ref. [13] for the maximum stable β_N as a function of aspect ratio and elongation.

The normalized beta β_N is either specified or taken as a fraction f_β of the stability limited β_N taken from Ref. [13].

$$\beta_N = \frac{f_\beta * 10 * \left(-0.7748 + 1.2869\kappa - 0.2921\kappa^2 + 0.0197\kappa^3\right)}{A^{0.5523} * \mathrm{TANH}\left[\left(1.8524 + 0.2319\kappa\right) / A^{0.6163}\right]} \quad . \tag{45}$$

Since the formula above gives the limiting beta as a function of aspect ratio and elongation and the elongation is also a function of aspect ratio, the use of the limiting expression above is especially apt for comparing various aspect ratio machines with constant proximity f_β to the aspect ratio varying beta limit.

The internal inductance is taken as 0.5 to correspond to the broad current profiles for the maximum beta equilibria in Ref. [13] but the value of ℓ_i plays little or no role in the calculations.

A bootstrap fraction f_{bs} is specified. The poloidal beta is then calculated according to

$$\beta_p = f_{bs} A^{1/2} / C_{bs} \quad , \tag{46}$$

with the constant C_{bs} taken as 0.75 for rough agreement with ONETWO plasma transport code calculations [5].

The toroidal beta is obtained from the equilibrium relation.

$$\beta_T = 25\left(\frac{1+\kappa^2}{2}\right)\left(\frac{\beta_N}{100}\right)^2 \frac{1}{\beta_p} \quad . \tag{47}$$

The scaled plasma current is calculated.

$$\frac{I}{a\,B_T} = 100\,\beta_T / \beta_N \quad . \tag{48}$$

The absolute plasma current is calculated

$$I_p\,(\mathrm{MA}) = a\,B_T\left(\frac{I}{a\,B_T}\right) \quad . \tag{49}$$

The toroidal field was determined in the toroidal coil section above generally by adjusting the TF current density to achieve a desired peak neutron wall loading at the outer midplane.

The poloidal magnetic field is

$$B_{pol} = \frac{0.2\,I_p}{a\left(\frac{1+\kappa^2}{2}\right)^{1/2}} \quad . \tag{50}$$

and the safety factor from the formula used by ITER is

$$q_{95\mathrm{ITER}} = \frac{(1.17-0.65\varepsilon)5a^2\,B_T}{\left(1-\varepsilon^2\right)^{5/2} R_0\,I_p}\,\frac{\left[1+\kappa^2\left(1+2\delta^2-1.2\delta^3\right)\right]}{2} \quad . \tag{51}$$

Density and temperature profiles are assumed parabolic.

$$n_e(r) = n_e(0)(1-r^2/a^2)^{S_N} \quad , \tag{52}$$

$$T_e(r) = T_e(0)(1-r^2/a^2)^{S_T} \quad . \tag{53}$$

The central ion temperature is specified as is the ratio of T_e/T_i.

The product of density and temperature can be calculated from beta.

$$n_e(0)T_i(0) = \frac{\left(1 + S_N + S_T\right)\beta_T B_T^2}{0.0403\left(T_e/T_i + f_{IMP} + f_i + f_{He}\right)} \quad . \tag{54}$$

The density is then derived from the above product

$$n_e(0) = \left[n_e(0)T_i(0)\right]/T_i(0) \quad , \tag{55}$$

and compared to the Greenwald density limit.

$$n_{GR} = I_p/(\pi a^2) \quad . \tag{56}$$

The average density is

$$\bar{n}_e = \frac{n_e(0)}{1 + S_N} \quad . \tag{57}$$

The stored energy is

$$W = \frac{3\beta_T V_p B_T^2}{1.6\pi} \quad . \tag{58}$$

Impurity Effects

The helium ion generation is calculated from the alpha power (see below for the alpha power calculation).

$$\dot{N}_{He}(\#/\text{sec}) = \frac{P_{ALPHA}}{3.52(1.6 \times 10^{-19})} \quad . \tag{59}$$

The ratio of helium confinement time to the energy confinement time is specified, generally as 10. The steady-state helium density is calculated.

$$n_{He} = \frac{\dot{N}_{He}\tau_{He}^*}{V_p} \quad . \tag{60}$$

The fraction of helium ions is then $f_{He} = n_{He}/\bar{n}_e$. However, to avoid circular references in the calculations, a fixed f_{He} is used and then checked after the fact for consistency with the above.

Neon is assumed as a radiating impurity with $Z_{IMP} = 10$ and the fraction that is neon ions is taken as $f_{IMP} = 0.01$, a value that usually produces copious neon radiation.

With these impurity assumptions, the fuel ion fraction in the plasma is

$$f_i = \frac{1 - 2\,f_{He} - f_{IMP}\,Z_{IMP}}{Z_i} \quad , \tag{61}$$

and that value is typically around 0.7. Since the fusion power is proportional to this value squared, the fusion power is 49% of what would be produced in a pure plasma. This is a conservative assumption. The Z_{eff} is

$$Z_{eff} = f_i + 4\,f_{He} + Z_{IMP}^2\,f_{IMP} \quad , \tag{62}$$

and is about 2, again a conservative value at the very high densities FDF will run at.

The fraction of the power in the plasma core that is radiated f_{RAD} is specified at 0.42.

The Brehmsstrahlung power is explicitly calculated and is generally about 10% of the power in the core plasma.

$$P_{BREHM} = \frac{0.00534\,V_p\,Z_{eff}\,n_e^2(0)\left[T_e(0)\right]^2}{1 + 2\,S_N + 0.5\,S_T} \quad . \tag{63}$$

An approximate treatment of the H-mode pedestal is implemented. The EPED1 first principles pedestal model [5,14–17] implies an approximate normalized beta at the pedestal top of 1.0. Then

$$\beta_{TPED} = \frac{\beta_{NPED}\,I}{100\,a\,B_T} \quad , \tag{64}$$

$$\beta_{PPED} = 0.25\,\beta_{NPED}\left(\frac{1+k^2}{2}\right)\frac{a\,B_T}{I_p} \quad . \tag{65}$$

The pedestal density temperature product $n_{PED}\ T_{PED}$ can be obtained

$$n_{PED}\,T_{PED} = \frac{\beta_{TPED}\,B_0^2}{0.0413\left(T_e/T_i + f_{imp} + f_{He} + f_i\right)} \quad . \tag{66}$$

The pedestal width from the EPED1 model is 0.08 $\beta_{PPED}^{1/2} = W_{PED}$.

The pedestal density is

$$n_{PED} = \eta_e(0)\left[1 - \left(1 - W_{PED}\right)^2\right]^{S_N} \quad . \tag{67}$$

The pedestal temperature is then $T_{ePED} = (n_{PED}\,T_{PED})\,n_{PED}$.

We also calculate the neoclassical offset counter rotation [18,19] associated with applied non-resonant error fields and compare it to the Alfven rotation frequency to assess the prospects for resistive wall mode stabilization by this rotation. We calculate local q at a specified r/a (generally 0.5).

$$q = \left[q_{95} - \left(\frac{1}{\ell_i^{0.7}} \right) \right] \left(\frac{r}{0.95a} \right)^{(4/\ell_i)} \frac{1}{\ell_i^{0.7}} \quad , \tag{68}$$

$$\omega_{offset} = \frac{2 \cdot K_c q S_T T_i(0) \left[1 - \left(\frac{r}{a} \right)^2 \right]^{S_T - 1}}{B_0 (A + Z_{eff}) a^3} \quad , \tag{69}$$

$$\omega_{ALFVEN} = \frac{B_0}{1000 R_0 \left\{ 2 \times 2.1 \times 10^{-13} n_e(0) \left[1 - \left(\frac{r}{a} \right)^2 \right] \right\}^{S_N}} \quad . \tag{70}$$

The offset rotation is often around 1% of the Alfven rotation, indicating potential for RWM stabilization since the threshold for that is likely to be less than 0.3% ω_{ALFVEN} [20].

II.F. CURRENT DRIVE SECTION

A bootstrap fraction f_{bs} is specified. The poloidal beta is then calculated according to

$$\beta_p = f_{bs} A^{1/2} / C_{bs} \quad , \tag{71}$$

with the constant C_{bs} taken as 0.75 for rough agreement with ONETWO calculations [5]. The total current that must be driven by auxiliary power is

$$I_{DRIVEN} = I_p (1 - f_{bs}) \quad , \tag{72}$$

The power required to drive the current by various means are calculated from formulae originally published by Tonon [8,21] but calibrated to calculations with ONETWO [5], NFREYA [22], TORAY-GA [23], and GENRAY [24]. For positive ion neutral beams which do not penetrate far beyond the pedestal top,

$$g_{NB} = 0.025 (\overline{T}_e) \quad , \tag{73}$$

$$P_{CDNBI} = \frac{n_{PED} R_0 I_{DRIVEN}}{0.018 T_{ePED}} \quad . \tag{74}$$

For fast waves,

$$g_{FW} = \frac{0.063 \overline{T}_e (1 + 0.5 \beta_T)}{2 + Z_{eff}} \quad , \tag{75}$$

$$P_{CDFW} = \overline{n}_e R_0 I_{DRIVEN} / g_{FW} \quad . \tag{76}$$

For Lower Hybrid waves,

$$n_{LHACC} = 0.12 B_T^2 \quad , \tag{77}$$

$$g_{LH} = \frac{0.037 B_T \overline{T}_e}{\left(5 + Z_{eff}\right) \overline{n}_e^{0.33}} \quad , \tag{78}$$

$$P_{CDLH} = \overline{n}_e R_0 I_{DRIVEN} / g_{LH} \quad . \tag{79}$$

For EC waves,

$$g_{EC} = 0.09 \overline{T}_e / (5 + Z_{eff}) \quad , \tag{80}$$

$$P_{CDEC} = \overline{n}_e R_0 I_{DRIVEN} / g_{EC} \quad . \tag{81}$$

The ECCD current is assumed driven at the plasma's half radius and so the average values of temperature and density are used. For the overall power balance calculations in the spreadsheet, we typically use $60\% \ P_{CDLH} + 40\% \ P_{CDEC}$.

The various EC resonance frequencies and cutoff densities for the first and second harmonic O-mode and the first harmonic X-mode are calculated.

$$f_{EC0} = 28 B_T \quad , \tag{82}$$

$$f_{EC2} = 2 f_{EC0} \quad , \tag{83}$$

$$n_c^{01} = B_T^2 / 10.3 \quad , \tag{84}$$

$$n_c^{02} = (2 B_T)^2 / 10.3 \quad , \tag{85}$$

$$n_c^{\times 1} = 2 B_T^2 / 10.3 \quad . \tag{86}$$

The total auxiliary power P_{AUX} is taken as a specified minimum value or the current drive power, whichever is greater.

$$P_{AUX} = P_{CD} \text{ if } P_{CD} > P_{AUX}^{SPEC}$$

$$= P_{AUX}^{SPEC} \text{ if } P_{CD} < P_{AUX}^{SPEC} \quad . \tag{87}$$

II.G. FUSION POWER AND DEVICE EFFICIENCY

An EXCEL macro performs the integral over the profiles of the fusion reactivity weighted by local density and temperature. This is the only 1-D calculation implemented. This integral must be done to get sufficient accuracy in the fusion power because it varies so strongly with local plasma parameters.

$$F.I. = \int_0^1 \left[\frac{n(x)}{n(0)}\right]^2 \frac{\overline{(\sigma v)}}{T_0^2}\, x\, dx \quad . \tag{88}$$

The fusion reactivity σv is taken from Ref. [25].

The fusion power and the alpha power are then

$$P_F = 7.043 \times 10^{15} (2V_p) f_i^2 \left[n_e(0) T_i(0)\right]^2 \times F.I.$$

$$P_\alpha = P_F / 5 \quad . \tag{89}$$

The plasma gain or Q is the ratio of the fusion power to the total auxiliary power.

The area of the blanket surface is

$$A_{WALL} = 4\pi^2 R_0 (1.05\, a)^2 \left(\frac{1+\kappa^2}{2}\right)^{1/2} \quad . \tag{90}$$

The peak neutron power at the blanket at the midplane is then $1.33 * 0.8 * P_F / A_{WALL}$, where the peaking factor 1.33 comes from 2-D calculations using a neutron source distributed according to typical density and temperature profiles over the plasma volume in actual tokamak geometry [5]. This is a most important quantity since it is typically used as a constant constraint to normalize across a range of machine designs.

Calculations are in the spreadsheet to estimate the efficiency and overall power gain of the candidate systems.

The electrical efficiency of the current drive system is taken typically as $\eta_{CD} = 0.4$ and the total electric power for the auxiliary systems is then

$$P_{AUX}^{EL} = P_{AUX} / \eta_{CD} \quad . \tag{91}$$

Finite efficiency of the DC power supplies for the TF and PF coils (generally 0.9) are usually taken into account.

The total thermal power generated is

$$P_{THERM} = M_B (P_F - P_\alpha) + f_{dis}\left(P\alpha + P_{AUX}^{EL} + P_{TF}^{EL}\right) \quad , \tag{92}$$

where M_B is the multiplication factor in the blankets owing to nuclear reactions, generally 1.25 and the second term envisions possibly capturing some of the first wall, auxiliary, and TF power into the thermal cycle. Of these, of course, only the alpha power and the auxiliary power extracted through the plasma facing components are likely to produce high grade heat suitable for the thermal cycle. The gross electric power generated assumes typically a 33% conversion of thermal power to electric power.

$$P_{GROSS}^{EL} = 0.33 P_{THERM} \quad . \tag{93}$$

The general house power to run the physical plant is taken as 7% of the gross electric power. Then the total power to run the plant is

$$P_{PLANT} = P_{AUX}^{EL} + P_{TF}^{EL} + P_{PF}^{EL} + P_{HOUSE} \quad . \tag{94}$$

The net electric power is

$$P_{NET}^{EL} = P_{GROSS}^{EL} - P_{PLANT} \quad , \tag{95}$$

and is negative for copper coil machines. To treat superconducting machines, we take as zero the TF and PF coil power. The plant gain or Q is

$$Q_{PLANT} = P_{GROSS}^{EL} \big/ P_{PLANT} \quad , \tag{96}$$

and is of course less than one for copper coil machines.

II.H. CONFINEMENT TIMES

At this point the plasma stored energy, the total auxiliary power, the alpha power, and all the plasma parameters are known so one can evaluate the energy confinement time required for power balance and compare it to various scaling rules and derive H factors.

$$\tau_E = W / P_{HEAT} \quad . \tag{97}$$

Since most scalings that have been constructed neglecting core line radiation, we construct the corresponding transport power, but subtract off explicitly only the Brehmsstrahlung power, which is a new feature of a burning plasma,

$$P_{TRANSP} = P_{HEAT} - P_{BREHM} \quad . \tag{98}$$

The confinement time required is then

$$\tau_{ENET} = W / P_{TRANSP} \quad . \tag{99}$$

The confinement time predicted by ITER89P L-mode scaling, ITER98y2 H-mode scaling, and the scaling that is correct in dimensionless parameters derived by Petty [26] are:

$$\tau_{89P} = 0.048\, I_p^{0.85} R_0^{1.2} a^{0.3} \bar{n}_e^{0.1} B_T^{0.2} \times (2.5\kappa / P_{TRANSP})^{0.5} \quad , \tag{100}$$

$$\begin{aligned} \tau_{98Y2} &= 0.0562\, I_p^{0.93} B_T^{0.15} P_{TRANSP}^{-0.69} \\ &\times (10\,\bar{n}_e)^{0.41} (2.5)^{0.19} R_0^{1.97} A^{-0.58} \\ &\times \kappa^{0.78} \quad , \end{aligned} \tag{101}$$

$$\begin{aligned} \tau_{PETTY} &= 0.028\, I_p^{0.83} B_T^{0.07} (10\,\bar{n}_e)^{0.49} \\ &\times P_{TRANSP}^{-0.55} R_0^{2.11} A^{-0.3} \kappa^{0.75} (2.5)^{0.14} \quad . \end{aligned} \tag{102}$$

The ratio of the needed confinement time to the scaling prediction is the H factor for the scaling of a given name.

II.I. DIVERTOR SECTION

Parameters to estimate the peak divertor heat flux are based on observations from DIII-D and the ITPA database. The scrape-off layer width for heat flow is taken from Loarte's analysis of the ITPA database [27].

$$\lambda_q = 0.00265 \times P_{HEAT}^{0.38} B_0^{-0.71} q_{95}^{0.3} \quad . \tag{103}$$

The heat flux is assumed to fall off exponentially in the SOL according to the width parameter. The flux expansion at the divertor strike points is taken as 4. The power into the scrape-off layer (SOL) is

$$P_{SOL} = P_{HEAT} - P_{RAD} - P_{BREHM} \quad , \tag{104}$$

where the heating power is the sum of the alpha power and the auxiliary power.

The P/R values P_{SOL}/R_0, P_{HEAT}/R_0 are calculated. The tilt angle θ between the field lines and the divertor plate in a poloidal plane is specified = 10 deg. The number of divertors

is generally taken $N_D = 2$ for double null operation. The fractions of power to the inner divertor and outer divertor are taken as $F_{ID} = 0.14$ and $F_{OD} = 0.86$. The wetted area of either both outer or both inner divertors is

$$WA = \frac{N_D\, 2\pi R_0\, (SOLW)\, F_x}{\sin(\theta)} \quad . \tag{105}$$

Peak heat fluxes to the inner and outer divertors and a gross value neglecting the in/out split are calculated.

$$\begin{aligned} \mathcal{P}_{SOL}^{IP} &= P_{SOL}\, F_{ID} / WA \\ \mathcal{P}_{SOL}^{OP} &= P_{SOL}\, F_{OD} / WA \\ \mathcal{P}_{SOL}^{P} &= P_{SOL} / WA \quad . \end{aligned} \tag{106}$$

Note that these peak heat fluxes do not take into account any radiation in the SOL or divertor plasmas and hence are conservative estimates, perhaps by a factor of two.

The poloidal extent of the wetted area is

$$L_{POL} = \frac{WA}{2\pi R_0} \quad . \tag{107}$$

The whole poloidal circumference is

$$C_{POL} = 2\pi a \left(\frac{1+\kappa^2}{2} \right)^{1/2} \quad . \tag{108}$$

The fraction of the poloidal circumference that must be devoted to divertor hardware is then

$$F_{POL} = L_{POL} / C_{POL} \quad . \tag{109}$$

II.J. THE OPTIMIZER

The optimizer takes the EXCEL non-linear SOLVER and wraps it around the basic spreadsheet described above. The SOLVER in EXCEL allows a quantity to be maximized or minimized subject to a set of constraints. The function minimized was usually $0.85 * R_0 + 0.006 * P_{PLANT}$. The weights give about equal motivation to the SOLVER to minimize the machine size and the total power dissipation in the facility. The constraints used in various combinations are described in Table I.

Table I
Constraints used in the Non-Linear Optimizer to Generate Designs that Minimize Machine Size and Power Consumption

- The ratio of auxiliary power to current drive power between 1 and 2.
- The water temperature rise in the TF centerpost less than 100°C. (The temperature rise seldom is more than 10°C owing to the very massive coils being laid out to keep reasonable the total facility power.)
- The peak neutron wall loading at the outer midplane equal to a specified value, generally 1.0 or 2.0 MW/m^2.
- The confinement quality H-ITER98y2 less than a specified value, generally 1.6.
- The density in relation to the Greenwald limit less than 0.8.
- The peak Von Meis stress in the TF coil equal to a specified value, generally 276 MPa (40 ksi).
- The fraction of the flux needed to ramp up the plasma current to full value provided by the OH solenoid half-swung equal to a specified value, generally 1.0.
- The peak hoop stress in the OH solenoid equal to a specified value, generally 228 MPa (33 ksi).

The free parameters the SOLVER is allowed to adjust to satisfy all these constraints and to minimize the size and power consumption of the machine are: the radial build of the TF coil centerpost, the current density in the TF coil, the radial build of the OH solenoid, the current density in the OH solenoid, and the ion temperature.

The optimizer spreadsheet varies the machine aspect ratio for a given machine concept in steps from 5 to 1.2 and for each aspect ratio constructs the optimum machine as above. The result is a set of graphics of machine parameters versus aspect ratio. Since the formula for β_N takes a fixed fraction of the beta limit calculated as a function of aspect ratio and since other physics constraints are put in terms of dimensionless quantities like the confinement H-factor and the ratio to the Greenwald density limit, the result is a set of machines versus aspect ratio that are constructed with constant physics assumptions and also constant hardware constraints. This allows a choice of the optimum aspect ratio among machines constructed on the same basis.

III. TWO INTERESTING FNSF CANDIDATES

Using the tools described in Section II, we have investigated the optimum aspect ratio choice for two different machine concepts. Each case is investigated versus aspect ratio using its own spreadsheet generally constructed as in Section II but customized to the particular machine concept. Both of these would be candidates for what has been generically named the Fusion Nuclear Science Facility (FNSF).

1. **FDF.** A conventionally constructed copper coil tokamak with an inboard breeding blanket and OH solenoid to drive the plasma current up to full value. The premise of this machine is that it be based on conventional tokamak construction approaches and presently known (or confirmable in 3 years) physics; i.e., it is a machine we could start to build essentially now. We find the optimum machine is at aspect ratio 3.5. We call such a facility a Fusion Development Facility. Since it is based on (conservative) Advanced Tokamak physics, it has been referred to as the FNSF-AT. It is a research machine optimized for the study and development of fusion blankets. We have extensively discussed such a machine and its mission scope in the last 3 years [3–5] and will only recap here the main mission components. The top level goal is to:

   Show fusion can produce energy and its own fuel.

Supporting goals are to:

- Produce significant fusion power (100–300 MW).
- Demonstrate fusion fuel self-sufficiency.
- Show fusion can produce high grade process heat and electricity.
- Provide a materials irradiation facility to develop low activation, high strength, high temperature, radiation resistant materials.
- Enable research on high performance, steady-state, burning plasmas for Demo.
- Obtain first data on fusion system operation, fuel management, reliability, availability, and maintainability to guide future fusion energy development.

FDF will accomplish these goals by operating steady-state with

- Modest energy gain ($Q < 7$).
- Continuous operation for 30% of a year in up to two-week-long periods.
- High neutron fluence (3–6 MW-yr/m^2).

2. **ST-CTF.** There has been much discussion of a Component Test Facility based on the copper coil Spherical Tokamak. Such a machine has also been referred to as the FNSF-ST. We applied our design tools to the ST-type machine and find an optimum aspect ratio of 1.7. The machine we arrived at is, in general, confirmatory of the results of the ORNL group [8,9]. The mission scope of the ST-CTF is very similar to

the FDF — at least in terms of the fusion nuclear science aspects. The ST-CTF we will present uses essentially the same conservative AT physics assumptions as the FDF. However, the ORNL group has positioned their ST-CTF such that no AT physics is used in its baseline operation. The resulting machine is somewhat larger than what we present. The ST-CTF is roughly half the major radius of the FDF and makes less fusion power. It may not be able to achieve actual net tritium production. It has two feasibility issues: startup without an OH transformer and quite high peak divertor heat flux (from its small size). Hence the start of construction of such a facility requires resolution of these two issues. But it is our view that with proper focus and effort in the U.S. experimental program these issues could be resolved in the same few years time scale envisioned for adequate resolution of the physics aspects of FDF. Hence this facility is also competitive in time as a realistic choice.

III.A. THE FUSION DEVELOPMENT FACILITY (FDF)

These machines are all based on conventional tokamak construction. Multi-turn TF centerposts are envisioned (with insulators between the slab-constructed turns). OH solenoids provide enough volt-seconds half-swung to run the plasma current up to full value. Construction of the TF and OH coils with conventional organic insulators determines the required inboard blanket/shield thickness (see neutronics section). At each aspect ratio the optimizer was allowed to vary the radial build of the TF coil and the current density in it, the radial build of the OH solenoid and the current density in it, the central ion temperature, and the fraction of the TF coil that is copper in order to achieve a cooling water temperature rise in the TF coil less than 100°C, a peak neutron wall loading at the outer midplane of 2 MW/m^2, confinement quality H98y2 less than 1.6, density ratio to the Greenwald limit less than 0.8, TF coil stress less than 276 MPa (40 ksi), OH stress less than 228 MPa (33 ksi), and enough OH flux half-swung to run the plasma current up to full value. The cost function minimized is that given in Section II, which equally emphasizes small machine size and small facility total power consumption. All machines are, of course, true steady-state with 100% non-inductive current drive. Results of the scan versus aspect ratio are given in the FDF-Cu curves in Figs. 3–11 (solid black line). In Fig. 3, one can see the minimum sized machine is at aspect ratio 3.5. However the minimum is very broad and we selected aspect ratio 3.5 as our optimum machine because the total facility power in that case came just under 500 MW (Fig. 4). Total facility power is always the design driver for copper coil tokamaks and we felt 500 MW was the largest value we could countenance. We describe in detail below the calculations given in the spreadsheet for this baseline case, taking it as typical of all the varied aspect ratio cases the optimizer considers.

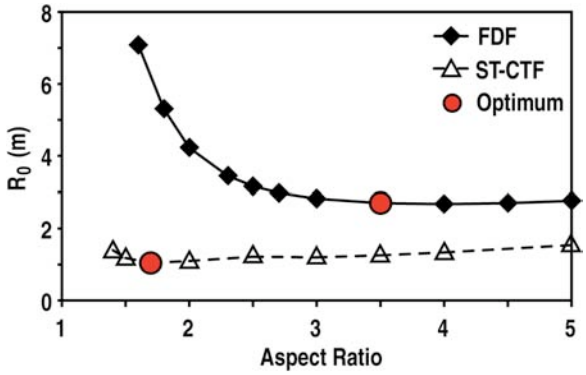

Fig. 3. Major radius versus aspect ratio for machines of the FDF and ST-CTF types.

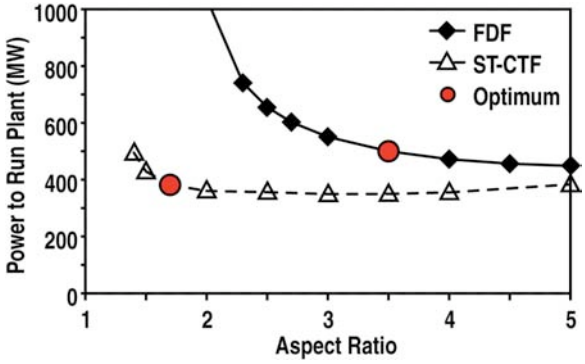

Fig. 4. Total facility power versus A.

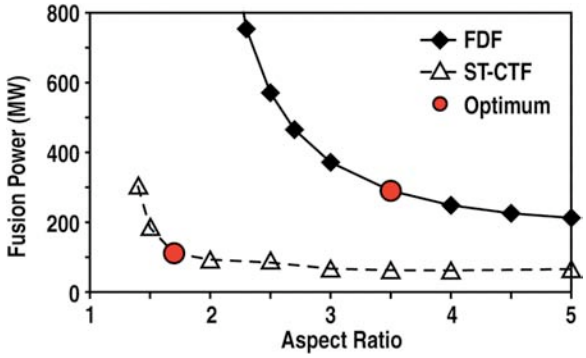

Fig. 5. Fusion power versus A.

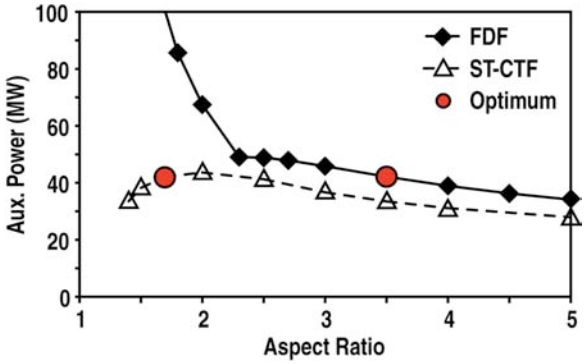

Fig. 6. Current drive power versus A.

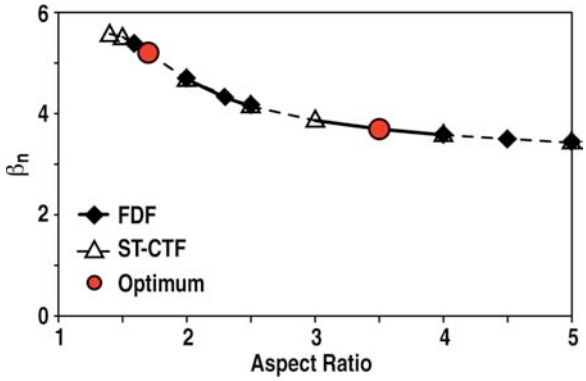

Fig. 7. The dependence of β_N on A common to all machines.

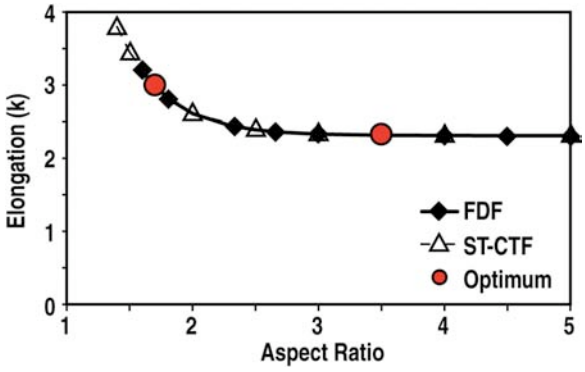

Fig. 8. The dependence of plasma elongation on A common to all machines.

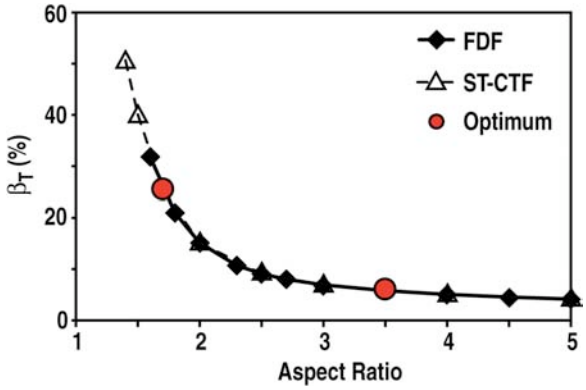

Fig. 9. Toroidal β versus A.

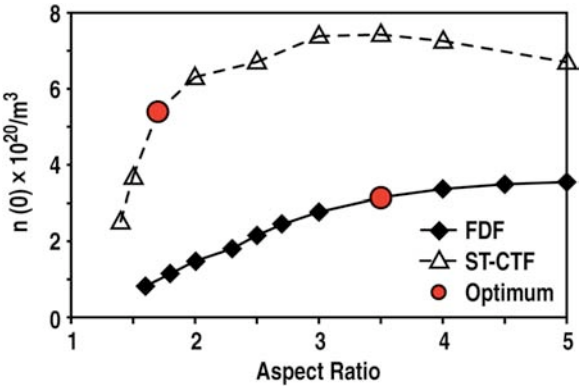

Fig. 10. Central electron densities versus A.

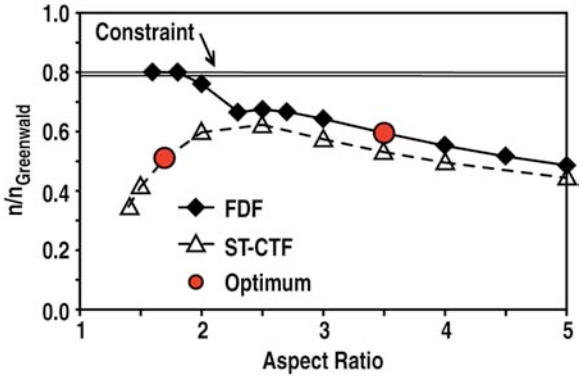

Fig. 11. Ratio of density to Greenwald limit.

III.A.1. FDF Baseline Geometry

Given the aspect ratio of 3.5, the elongation of 2.31 was obtained as 95% of the maximum stable elongation. An inner blanket thickness of 0.6 m and an outer blanket thickness of 0.8 m were assumed. These thicknesses were established by our design studies iterated with neutronics calculations (see Section III.A.10) to give net TBR > 1 and also allow the magnet coils to be constructed with ordinary organic insulators. The inner plasma gap was taken as 5 cm and the outer gap 8 cm.

The radial build of the TF coil selected by the optimizer is 1.183 m from the axis of symmetry of the machine and radial build of the OH solenoid wound on the TF centerpost is 0.098 m. Given these values, the major radius and the minor radius of the baseline case are determined to be $R_0 = 2.70$ m and $a = 0.77$ m. The baseline case is thus positioned between DIII-D and JET in size, albeit closer to JET than to DIII-D. Nevertheless, for such machines, we are not extrapolating physics a factor of two in size as was the case with ITER — we are interpolating in size. The current density in the toroidal coil of 16.7 MA-m^{-2} is determined

by the optimizer to give a peak neutron wall loading at the outboard midplane of 2 MW-m^{-2}. The toroidal field resulting from the determined TF geometry and the TF current density is 5.44 T. The TF stresses and cooling parameters then follow as in the formulae in the Toroidal Coil section above and set by the optimizer as constraints.

III.A.2. FDF Baseline Plasma Parameters

In the Plasma Parameters section, the value of normalized beta, β_N, is taken as 67% of the limiting β_N value calculated in Ref. [13]. The limiting value of β_N thus resulting was 3.69, which is equivalent to β_N = 3.3 in DIII-D at the same fraction of the beta limit since the aspect ratio of DIII-D is 2.7, the elongation is typically 1.7, and the limiting β_N scales approximately like $1/A^{0.5}$ and linearly with elongation. This is a conservative AT physics position since β_N = 3.3 has been achieved in DIII-D with no current driven by the ohmic heating transformer, utilizing ECCD and NBCD, and achieving a fully aligned current density profile [28]. This case had still a slowly evolving current profile owing to insufficient ECCD power to hold the current profile stationary and so terminated with a tearing mode. In the next few years, increased ECCD power and off-axis NBCD from tilted neutral beams should allow this operating mode to be extended to 5–10 s, a few current diffusion times, in true steady-state. Also β_N = 4 has been achieved in DIII-D with 100% non-inductive current drive, but in that case about 20% of the plasma current was driven by ramping the toroidal field to obtain significant off-axis current drive [29]. To extend this line of AT operation, increased ECCD and tilted neutral beams will at least partially replace the off-axis current from ramping the toroidal field. In principle, the off-axis current derived from TF ramping can also be replaced by LHCD, but that line of research is on Alcator C-mod. Most recently, DIII-D has also achieved fully non-inductive operation at β_N above 4.5 in the so-called high ℓ_i experiments [30]. Again increased ECCD and tilted neutral beams will enable further progress along this line toward true steady-state. The point is that DIII-D has three different operating modes already with 100% non-inductive current and which exceed the FDF baseline requirement in β_N. We feel that these three cases can be extended to true steady-state demonstrations in DIII-D within the next 2–3 years.

A fixed bootstrap fraction of 75% was selected and used in all cases. Bootstrap current 100% has been achieved in tokamaks [31]. Then the poloidal beta of 1.87 is calculated as above from the aspect ratio and the bootstrap fraction. Then since β_N and β_P are known, then the toroidal beta β_T = 5.8% is calculated from the equilibrium relation. The scaled plasma current, the actual plasma current, and the safety factor q immediately follow as in Section II. The plasma current is 6.6 MA and the ITER value of q_{95} is 5.0, a very safe value characteristic of steady-state, high beta machines.

Since the toroidal field and the β_T and the plasma geometry are known, an approximate fusion power could be calculated, but to get a more accurate fusion power calculation, the β_T must be broken up into density and temperature separately. The plasma β_T and toroidal

field and the impurity assumptions and the assumption on the ratio T_e/T_i = 1.0 and the assumed density and temperature profile shapes allow calculation of the density and temperature product. An ion temperature of 16.4 keV (again found by the optimizer) is selected. The high value promotes high current drive efficiency since most current drive efficiencies go like T/n. A conservative specification of impurity densities is made as described in Section II. The helium fraction was 5%. The resulting central density is 3.14 x 10^{20} m^{-3} and the average density is a safe 60% of the Greenwald density limit. The density profile was taken S_N = 0.5 as expected for future larger, high density, low collisionality machines [5]. The temperature profile was assumed more peaked S_T = 0.75. This value was chosen to give an overall pressure peaking of 1.0 + S_N + S_T = 2.25, the optimum value found by Garofalo [29] for maximizing n=1, 2 and 3 plasma stability to the resistive wall mode [14].

The density at the top of the H-mode pedestal is 1.0 x 10^{20} m^{-3} and the pedestal temperature is 5.94 keV. The predicted offset counter rotation from non-resonant error fields is 11.7 krad/s which is 0.6% of the Alfven rotation indicating this should be sufficient rotation for resistive wall mode stabilization, if this emerging physics picture of offset rotation holds together.

III.A.3. FDF Baseline Auxiliary Heating and Current Drive

Now that the density and temperature are known, the power required to drive the non-bootstrap current can be calculated. Since our supporting studies with the ONETWO transport code are heading toward machines with LHCD and ECCD and only a small NBI to drive edge rotation, we take the required current drive power as 60% of the LHCD value plus 40% of the ECCD value. To drive the remaining 25% of the plasma current, 42 MW is required.

The EC fundamental frequency is 152 GHz and the second harmonic is 305 GHz. The cutoff density for outside launch O-mode is 2.88 x 10^{20} m^{-3}, so the very plasma center would be cutoff for simple first harmonic outside launch O-mode; some further small (5–10%) adjustment may be needed here to make the plasma center visible. For reference, the cutoff density for second harmonic O-mode is 11.5 x 10^{20} m^{-3} and for inside launch fundamental X-mode is 5.8 x 10^{20} m^{-3}.

III.A.4. FDF Baseline Fusion Power

The fusion power is calculated by integrating the fusion reactivity over the plasma cross section thereby taking into account the profiles of density and temperature. The baseline case has a fusion power of 290 MW. The plasma energy gain Q is the ratio of the fusion power to the auxiliary power and is 6.9. With this modest but significant gain, alpha heating effects and the effects of alpha heating on the plasma profiles will be easily seen for study, but will not be so dominant in the plasma control. Hence FDF can make an important

contribution to alpha physics and progress toward controlling a burning plasma, but FDF does not compete for the high energy gain mission of ITER.

The peak neutron wall loading at the outer midplane is calculated using a peaking factor 1.3 derived from 2-D calculations of neutron fluxes from a neutron source distributed over the plasma volume according to local temperatures and densities. A neutron wall loading of 2 MW/m^2 is a specification for the baseline case. Given the fixed physics that is all derived essentially in deterministic lock step from the aspect ratio, the toroidal current density is adjusted to achieve the specified peak neutron wall loading. This is how the value of the toroidal field is determined.

III.A.5. FDF Baseline Toroidal Coil

From the geometry and the current density in the toroidal coil, the stresses in the TF coil centerpost are calculated. A peak hoop stress of 276 MPa is calculated. In fact, this value is a constraint used by the optimizer to examine sets of machines all with the same TF stress levels. The temperature rise in the cooling water is calculated to be just a few degrees centigrade with 10% of the cross-section devoted to water flow. Because the water flow path is short, just once through vertically, cooling the centerpost is never even close to a problem because to keep down the total facility power, the TF coils come out rather massive with low current densities.

The detailed layout of the TF coil is made as in the TF section. The overall height of the TF centerpost is 8.57 m and is the sum of the plasma height from X-point to X-point, twice an allowance of space for the divertor that is 25% of the minor radius, twice the thickness of the neutron shielding which is assumed to be 83% of the nominal inboard shield thickness, and twice the height of the radial wedge section.

The radial wedge sections are taken as 1.5 m in vertical height at the centerpost and 1.81 m at the return legs where they match onto half the toroidal circumference at the return legs. The radial thickness of the outer vertical return legs is determined by assuming a low 4 MA/m^2 current density in them. That thickness is 1.23 m.

The mass and power dissipation in the centerpost, the radial wedges, and the vertical return legs is given in Table II. Total TF power is 286 MW.

Table II
TF Coil Parameters for FDF

	Mass (1000 kg)	Power Dissipated (MW)
Centerpost	304	202
Radial wedges	1639	36
Return legs	2871	48

III.A.6. FDF Baseline OH Solenoid

The current density in the ohmic heating solenoid is chosen so that solenoid can provide all the volt-seconds needed to ramp up the plasma current to its full value by half-swung operation. To get to the plasma current of 6.6 MA, a flux from the solenoid of 27.3 V-s is needed. The radial build of the solenoid is 0.098 m and the current density in it is 46.4 MA/m^2. The stress in the solenoid is calculated to be 228 MPa (33 ksi) which is a constraint used by the optimizer to examine sets of machines all with the same OH stress levels. Somewhat lower stress is specified for the OH coil compared to the TF coil because the OH coils sees more demanding service.

In this spreadsheet, the solenoid is only considered as inertially cooled. It is considered that it will only be half-swung in steady-state operation so that it winds up near zero current during the long steady-state plasma current flattop so that the minimal cooling that can be provided will be adequate. In reality, the OH solenoid will be segmented to assist in plasma shaping so while the average current in this inner stack of coils may be near zero, individual coil currents may be of the order of 25% of full current. Within this frame work, the temperature rise produced in the solenoid by the triangle shaped current waveform in it (a linear ramp for charging and a linear ramp for discharging to start the plasma up) is evaluated assuming just the thermal mass of the solenoid. With an assumed maximum temperature rise of 50 deg centigrade, this relation is inverted to calculate the linear rise time allowed. For the baseline solenoid with mass 18,200 kg the rise time is 4.5 s. With some water cooling (to be considered in the future), this value might be perhaps doubled and would be reasonable. The necessary rate of rise of the plasma current to get to 6.7 MA in about 4.5 s is 1.5 MA/s, high but not out of range. With a doubling of the rise time with some cooling, this value would be cut in half and be quite within range of current tokamak experience. The maximum loop voltage is just 6.1 V, about what modern tokamaks use.

In principle, the OH solenoid could be double swung and produce twice the volt-seconds and double the plasma current. However, then the solenoid will be at full current for steady-state flattop with inadequate cooling for steady-state at that level. So the flattop can only be sustained for a few seconds perhaps until the OH solenoid must be turned off. But this double swung operation may be a way to access higher current, inductively driven, high energy gain plasmas for a few energy confinement times so FDF can make at least a short pulse contribution to high gain physics studies. There may also be a compromise position (to be worked out) in which the solenoid is swung forward to say half of full current and perhaps the steady-state cooling could support that level of current (one-fourth power) in steady-state. Then FDF could enable the study of fairly high energy gain plasmas in steady-state.

III.A.7. FDF Baseline PF Coils

A set of PF coils is laid out as in the PF coil Section II.D. The purpose of this layout is to get the masses and the power dissipation in a reasonable set of coils to go into the estimate of

total facility power required. In Table III, we give the radius, the area, the mass and the power dissipated in the up-down symmetric pairs of PF coils. Clearly, since PF2 is so much larger than PF1, further optimization of the outer PF system can be made after another round of equilibrium calculations. However, our purpose here is just to get an approximate value of the power contribution of the PF coils to the total facility power.

Table III
PF Coil Parameters for FDF

	Radius (m)	Area (m^2)	Mass (1000 kg) (1 of 2)	Peak Power (MW) (1 of 2)
PF1	1.992	0.438	49	18
PF2	4.356	0.673	165	10
PF3	4.538	0.132	34	3.6

III.A.8. FDF Baseline Energy Confinement Times

Given the heating powers calculated and the stored energy and the plasma parameters, the required energy confinement time of 0.84 s was calculated by the methods above. This energy confinement time is then divided by the various scaling law predictions to get the H-factor. An H-factor with respect to ITER's H-mode scaling, ITER98y2, is 1.6 and was a constraint implemented by the optimizer. This value is consistent with already achieved values ranging up to 1.7 for the longest duration discharges on DIII-D that run dozens of energy confinement times and a few resistive times. The ITER98y2 scaling is known to be wrong in terms of dimensionless parameter dependences. In particular, it implies confinement degrades almost linearly with increasing beta; whereas experiments in DIII-D and most machines imply no or weak beta dependence. Hence ITER98y2 punishes high beta machines like FDF and should be regarded as a conservative scaling. Petty's scaling incorporates correct dimensionless parameter dependences and is an equally good fit to the ITER confinement database. The H-factor against Petty's scaling is just 1.22, an extremely conservative value set against the typical value of 1.8 in long pulse discharges in DIII-D. The H-factor against ITER's L-mode scaling ITER89P is 2.96. While FDF is positioned using the conventional ITER98y2 scaling, this discussion implies FDF has been positioned conservatively in its confinement assumptions. First principles confinement calculations using the GLF23 confinement model have confirmed the confinement assumptions made for FDF [5].

III.A.9. FDF Baseline Divertor Heat Fluxes

The various parameters characterizing heat fluxes to the divertor were calculated using the methods described in Section II.H. The magnetic field of 5.44 T, safety factor of 5, and total heating power of 100 MW give a λ_q = 0.0074 m from Loarte's formula [1]. Two

divertors with flux expansion 4 and 10 deg plate tilt were assumed. The power into the SOL was 45 MW. While the raw P/R value is high, 37 MW/m, the anticipated peak heat flux on the outer divertor plate is just 6.7 MW-m^{-2}, a value we know can be engineered since ITER is engineering for 10 MW-m^{-2}. Peak heat flux to the inner divertor is 1.09 MW/m^2. These values neglect completely radiation in the SOL and divertor, which should reduce the peak heat flux a factor of 2–4. The peak heat flux can also be reduced by designing for more flux expansion and if the λ_q turns out larger. On the other hand, the peak heat flux would be increased by more plate tilt (20 deg – a factor 2), single null operation (factor 1.6 increase) or a smaller λ_q. The value P/R, while a useful characterization across machines with highly varying divertor geometries, is not an appropriate variable to scale with since peak heat flux involves one more machine dimension, details of how the divertor is designed, the magnetic geometry, and the radiation in the SOL and divertor. The peak heat fluxes in FDF are in a conservative range because the machine is not so small, between DIII-D and JET in size.

III.A.10. Shielding and Tritium Breeding Calculations for FDF

In this section, we describe the initial neutronics screening assessment that was carried out for our initial FDF baseline design which is a somewhat smaller machine with R = 2.49 m, a = 0.71 m, A = 3.5, 50 cm thick inboard and outboard blanket/shields, and a 25 cm shield for the divertor coils. We discuss how the results of this assessment led to the current baseline design. We calculated the inboard (IB) and outboard (OB) tritium breeding ratio (TBR), the peak He production for both the ferritic steel and SS316 structure considered in the analysis, the peak fast neutron ($E > 0.1$ MeV) fluence in the magnets, and the peak magnet organic insulator dose. The reweldability limit is 1 He appm. The limit on fast neutron fluence in the magnets is 10^{22} n/cm^2 for ceramic insulators. The peak absorbed dose limit for organic insulators in magnets is 10^{10} Rad.

The basic plan for FDF is to engineer the blanket/shield assembly as the structural element which will support a relatively thin vacuum boundary at the rear surface of it. We considered a 5 cm thick steel vacuum vessel region. The back plates were considered as part of the blanket/shield. We considered an OH coil right behind the 50 cm IB blanket/shield. Zones of Cu/steel/insulator mixture were used to represent the 8.5 cm thick OH coil. This was done to account for the shielding effect of the OH coil on the TF coil. Both magnets are normal copper magnets. We assumed that the OH coil is replaced every time the IB blanket/shield assembly is replaced which is at about one-third the overall machine lifetime. Hence, the OH coil has to survive the environment corresponding to 2 MW-yr/m^2 peak outboard neutron fluence. The TF coil behind the OH coil is considered to survive for the full lifetime of the facility that corresponds to 6 MW-yr/m^2 peak outboard neutron fluence. Note that the peak inboard fluence is about two-thirds the peak outboard fluence.

Many inboard blanket/shield design options with various materials were considered in our earlier study [3]. For the shield, we considered WC, B4C, SS316, and ferritic steel (FS)

with helium or water cooling. We looked at a non-breeding inboard shield sufficient for shielding the inboard OH coil and the TF coils. The coverage fraction for the inboard side is 10% to 20% depending on the machine aspect ratio. The impact on overall TBR can be minimized by using materials that help reflect neutrons to be utilized in outboard breeding. A possible approach that we investigated is to use a non-breeding steel shield with beryllium added in the front layers behind the first wall (FW). Without inboard breeding, we found that a marginally acceptable TBR (~1) can be obtained only if He/FS shield is used with modest enhancement (3%) obtained if 6 cm Be is added behind the FW. Using WC, B_4C, or H_2O in the IB shield, while improving the IB shielding, has a devastating effect on TBR. While ceramic insulators could be used with any of the design options, the OH coil could be made with organic insulators only if the IB 50 cm region was an optimized non-breeding shield made of H_2O/SS/WC. This leads also to a modest radiation induced resistivity increase of 2.2 nΩm (only ~1.4% increase for room temperature magnets). However, in that case the overall TBR is only ~0.6. If a breeding blanket is utilized in the full IB 50 cm space, a TBR>1 can be achieved but the lower shielding effectiveness of the breeding blanket would require the OH coil to use ceramic insulators. Therefore, design of IB blanket/shield assembly is a trade-off between magnet shielding and tritium breeding.

The option where a breeding blanket occupies the front part of the IB space followed by a WC/steel shield appears to be the best compromise between breeding and shielding requirements. Two blanket concepts were considered. The first was a dual coolant lead lithium blanket (DCLL) with FS structure cooled by He and PbLi (90% Li-6) breeder isolated from the structure by SiC Flow Channel Inserts (FCI); the DCLL radial build was provided by S. Malang [32]. The second was a helium-cooled ceramic breeder (HCCB) blanket with FS structure, He coolant, Be multiplier, and Li_4SiO_4 (80% Li-6) breeder and the radial build was provided by C. Wong [33]. The shield used behind the blanket is made of FS structure with WC filler. The two coolant options, helium and water, were considered. The composition of the shield is 15% FS, 70% WC, and 15% coolant. In both options an 8.5 cm OH coil consisting of 75% Cu, 10% spinel ($MgAl_2O_4$) ceramic insulator, and 15% H_2O is placed between the shield and the inboard leg of the TF coil. The results for these options are given in Table IV.

The results indicate that both shield options with the DCLL blanket yield reasonable TBR with slightly larger margin with helium cooling. Lower TBR obtained with the HCCB blanket. Using the HCCB blanket in place of the DCLL blanket with He-cooled shield results in slightly better shielding performance due to the larger steel content and moderating effect of the Be in the HCCB blanket. However, comparable results are obtained with the water-cooled shield where the water compensates for the lower amount of steel and moderator in the blanket. Rewelding the vacuum vessel (VV) is not an issue for all options if FS VV is used. Using water-cooled shield allows rewelding for VV even if it is made of SS316. Replacing He by water in the shield reduces the radiation parameters in the VV, OH,

and TF coils by factors of ~1.5–5. All options yield acceptable fluence for ceramic insulator when used in both OH and TF coils. The absorbed dose in the organic insulator exceeds the design limit for all options and both OH and TF coils. Despite the added 8.5 cm shielding by the OH coil, the end-of-life dose in the TF coil is similar to that in the OH coil which sees just one-third the facility lifetime fluence. Based on the calculated shield e-fold for organic dose, we estimated the additional shield thickness required to allow using organic insulators. In order to allow using organic insulators in both the OH and TF coils, the shield thickness should be increased by 8–23 cm depending on the design option chosen as indicated in Table IV.

Table IV
Blanket and Shield Option Analyses

IB Design Option	He-Cooled Shield		Water-Cooled Shield	
	DCLL	HCCB	DCLL	HCCB
IB TBR	0.25	0.23	0.23	0.22
OB TBR	0.93	0.83	0.92	0.83
Total TBR	1.18[(a)]	1.06	1.15	1.05
Peak He appm in SS VV	**1.68**[(b)]	0.80	0.31	0.29
Peak He appm in FS VV	0.10	0.15	0.07	0.11
Peak fast neutron fluence in OH coil (n/cm^2)	1.9×10^{20}	1.2×10^{20}	4.7×10^{19}	4.4×10^{19}
Peak organic insulator dose in OH coil (rads)	**2.1×10^{11}**	**1.1×10^{11}**	**4.6×10^{10}**	**4.4×10^{10}**
Peak fast neutron fluence in TF coil (n/cm^2)	7.3×10^{19}	6.2×10^{19}	2.9×10^{19}	3.3×10^{19}
Peak organic insulator dose in TF coil (rads)	**2.2×10^{11}**	**1.2×10^{11}**	**4.8×10^{10}**	**4.8×10^{10}**
Shield e-fold for organic insulator dose (cm)	7.6 cm	7.6 cm	5.5 cm	6.3 cm
Added shield for using organic insulator in OH coil	**~23 cm**	**~19 cm**	**~8 cm**	**~10 cm**
Added shield for using organic insulator in TF coil	**~23 cm**	**~19 cm**	**~8 cm**	**~10 cm**

[(a)]Gray shade = design limits or design goals achieved.
[(b)]**Bold = over design limits or under design goal.**

For the outboard side, the results are given in Table V. It is assumed that the full 70 cm OB space is occupied by the blanket. Notice that the OB VV and magnet parameters are not sensitive to the IB shield choice. Both blanket options provide adequate shielding for the VV if it is made of FS. If SS316 VV is used, ~5 cm shield should be added between the blanket and VV in case of DCLL blanket. The HCCB blanket provides significantly better magnet shielding than the DCLL blanket.

Table V
Outboard Neutronics Results

	DCLL	HCCB
Peak He appm in SS VV	**1.7**[(a)]	0.4[(b)]
Peak He appm in FS VV	0.1	0.1
Peak fast neutron fluence in magnet (n/cm^2)	1.8×10^{21}	1.3×10^{20}
Peak organic insulator dose in magnet (rad)	**1.3×10^{12}**	**1.9×10^{11}**
Added He-cooled shield to use organic insulators	**~37 cm**	**~23 cm**
Added H_2O-cooled shield to use organic insulators	**~27 cm**	**~19 cm**

[(a)]**Bold = over design limits or under design goal.**
[(b)]Gray shade = design limits or design goals achieved.

The OB magnets are well shielded by either blanket if ceramic insulators are used. If organic insulators are used, 19–37 cm shielding should be added depending on the blanket and shield used. Based on these results, we elected to add just 10 cm to a total of 80 cm for the OB blanket/shield assembly considering that the PF coils and other structures on the outboard side will provide significant shielding for the TF coil. The PF coils can have additional shielding placed around them; indeed their cases shield the insulators inside. Finally the peak neutron flux occurs at the midplane and the PF coils are well off midplane where the neutron wall loading is smaller and the blanket much thicker. Eventually 3-D calculations will have to be made to pin down the outboard side shielding.

Simple fall-off distances for nuclear effects were obtained to enable simple rescaling in the spreadsheet work. These are given in Table VI but must be used with caution. We used the above calculations as a baseline and the e-fold distances for attenuation in different materials to estimate the shielding needed. Based on this, we concluded that if organic insulators are used in OH ad TF coils, a 60 cm IB radial build that is divided equally between either of the blanket options and a water cooled FS/WC shield, should be used. The total OB blanket/shield radial build is 80 cm. This is divided to either 45 cm DCLL blanket and 35 cm water cooled FS/WC shield or 50 cm HCCB blanket and 30 cm water cooled FS/WC shield. The TBR is acceptable with DCLL blanket but is marginally acceptable with HCCB blanket. We used the information in Table VI to estimate the shielding required to protect the divertor coil. From these considerations and the lower neutron wall loading in the divertor regions, we increased the blanket/shield thickness between the divertor coils and the plasma to 50 cm so that organic insulators can be used. These inboard, outboard, and divertor region changes resulted in making the machine bigger and led to the new rebaselined FDF design with R = 2.70 m. These initial scoping calculations have been done with uniform cylindrical models, neglecting 3-D aspects such as ports and divertor pumping ducts. Detailed 3-D analysis is

underway for the new baseline to confirm that this configuration including ports and pumping ducts provides adequate tritium breeding while satisfying all radiation shielding requirements.

Table VI
e-folding Distances for Attenuation of Neutron Effects through Various Materials

	Fast Neutron Flux	FS He Production	Organic Insulator Dose
HCCB blanket (facing plasma)	11.5	9.1	11.7
DCLL blanket (facing plasma)	18.8	12.7	16.6
WC/He shield (behind HCCB)	9.4	6.2	7.6
WC/He shield (behind DCLL)	7.0	6.2	7.6
WC/H2O shield (behind HCCB)	6.7	5.9	6.3
WC/H2O shield (behind DCLL)	5.0	5.7	5.5

Finally to enable some consideration of superconducting fusion reactors, we developed a simple methodology to estimate local and volume-integrated nuclear heating in the TF centerpost. The nuclear heating for a copper TF coil is negligible compared to the ohmic heating. But it is an important limit for superconducting coil machines like ARIES-AT. The actual limit for superconducting coils is not a limit on power density (W/cm^3) in the coil; it is a limit on the total integral nuclear heating in the superconducting centerpost which arises from the largest affordable single unit liquid helium refrigerator. As a result, it is usually assumed that the centerpost nuclear heating must be kept below 17 kW.

The neutronics assessment provided us with the values needed to calculate nuclear heating in the TF centerpost. For the case of a 2 cm PFC followed by a 23 cm DCLL blanket followed by a 25 cm H_2O cooled FS shield with WC filler followed by an 8.5 cm thick OH coil, we calculated the nuclear heating at the midplane at the outer surface of the TF coil to be 0.035 W/cm^3, a normalizing value we will call M_0. This value is normalized to 2 MW/m^2 neutrons flux at the outer midplane and about two-thirds of that at the inboard midplane. We developed perturbations around this result to consider alternative shield thicknesses.

Let S(cm) be the total thickness of blanket, shield and OH coil. Then the nuclear heating density at the TF coil is denoted M_c and is

$$M_c = M_0 \exp\left[-\left(S-58.5\right)/\lambda\right] \quad . \tag{110}$$

We take the attenuation length for nuclear heating to be the e-folding length for energetic neutrons from the e-folding table (Table VI) for H_20 cooled FS shielding. Then λ = 5.5 cm.

We assume the nuclear heating density M varies in the TF centerpost according to

$$M = M_c \left[1 - Z/h\right] \exp\left(-x/\lambda_{TF}\right) \quad , \tag{111}$$

where Z is the height above the midplane, h_c is the height of centerpost exposed to nuclear heating, and λ_{TF} is the falloff length for nuclear heating going a depth x into the TF centerpost. So we have a linear falloff with height from the midplane to half the value at the end of the centerpost. This is a reasonable model. The value λ_{TF} we take as 8 cm.

Then the total nuclear heating is

$$TFH = M_c \int_0^{0.5\,hc} 2\left[1 - Z/h_c\right] dZ * \int_0^D 2\pi\left(R_c - x\right)\exp\left(-x/\lambda_{TF}\right) dx \quad , \tag{112}$$

where D is the depth into the centerpost. We might take D to infinity later. R_c is the outer radius of the centerpost. The integral is

$$\begin{aligned} TFH = {} & 0.75\, M_c\, h_c\, 2\pi \left\{ R_c \lambda_{TF} \left[1 - \exp\left(-D/\lambda_{TF}\right)\right] \right. \\ & \left. - \lambda_{TF}^2 \left[1 - \left(1 + D/\lambda_{TF}\right)\exp\left(-D/\lambda_{TF}\right)\right] \right\} \quad . \end{aligned} \tag{113}$$

The value integrating to an infinite depth into the centerpost is

$$TFH = 0.75\, M_c\, h_c\, 2\pi \left(R_c \lambda_{TF} - \lambda_{TF}^2 \right) \quad . \tag{114}$$

III.A.11. Various Operating Modes and Potential for High Q Operation

It is important to realize and have clearly in view that any research tokamak like FDF has a variety of operating modes. Some of the operating modes for FDF are summarized in Table VII.

The baseline operating mode of FDF has been extensively described above and its intent is to provide a peak neutron flux at the outer midplane of 2 MW-m^{-2} utilizing what we have characterized as conservative Advanced Tokamak physics. Operating for 10 years at duty factor 0.3, this mode would accumulate 6 MW-yr/m^2 fluence.

Lesser Performance Modes that Preserve the Nuclear Science Mission

Few machines ever operate at their high end of performance all the time. While the baseline case is not even the top end of FDF's capability, it is useful to assure that the mission of FDF to develop fusion's nuclear technology is secure if lower performance than the baseline is realized. To that end, the column headed. "Lower B, fbs 1.0 MW-m^2" was created. In this operating mode with reduced toroidal field (3.9 T) and 56% bootstrap fraction, a peak neutron flux of 1.0 MW-m^{-2} at the outboard midplane is still created. This flux of neutrons would still be quite adequate for the development of blankets. The 10-year fluence accumulated would still be 3 MW-yr/m^2, still a significant fluence. Considering this

Table VII
FDF Operating Modes

			Baseline 2 MW/m^2	Lower B, fbs 1.0 MW/m^2	Lower β_N fbs, H98	Advanced	Very Advanced
A	Aspect ratio		3.5	3.5	3.5	3.5	3.5
a	Plasma minor radius	m	0.77	0.77	0.77	0.77	0.77
R_0	Plasma major radius	m	2.70	2.70	2.70	2.70	2.70
k	Plasma elongation		2.31	2.31	2.31	2.31	2.31
J_c	Centerpost current density	MA/m^2	16.7	12.0	16.7	16.7	16.7
P_f	Fusion power	MW	290	145	159	476	635
$P_{internal}$	Power to run plant	MW	500	348	527	501	492
Q_{plasma}	P_{fusion}/p_{aux}		6.9	3.5	2.9	12.4	19.8
P_n/A_{wall}	Neutron power at blanket	MW/m^2	2.0	1.0	1.1	3.3	4.4
β_T	Toroidal beta		0.058	0.078	0.041	0.076	0.088
β_N	Normalized beta	mT/MA	3.69	3.69	2.65	4.50	5.00
f_{bs}	Bootstrap fraction		0.75	0.56	0.54	0.85	0.90
P_{cd}	Current drive power	MW	42	41	54	39	32
I_p	Plasma current	MA	6.60	6.39	6.56	7.09	7.43
B_0	Field on axis	T	5.44	3.90	5.44	5.44	5.44
TF Stress	Stress in TF coil	MPa	276	142	276	276	276
q	Safety factor		5.00	3.70	5.02	4.65	4.43
$T_i(0)$	Ion temperature	keV	16.4	18.2	16.4	15.0	15.5
$n(0)$	Electron density	E20/m^3	3.14	1.96	2.22	4.32	5.11
$\bar{n}/n_{GR}$	Ratio to Greenwald limit		0.60	0.38	0.42	0.76	0.86
Z_{eff}			2.00	1.98	1.96	2.02	2.03
W	Stored energy in plasma	MJ	73	51	52	96	112
P_{AUX}	Total auxiliary power	MW	42	41	54	39	32
τ_E	τ_E	sec	0.73	0.73	0.61	0.72	0.70
HITER98Y2	H factor over ELMY H		1.60	1.60	1.36	1.60	1.60
P_{SOL}/A_{div}	Peak divertor heat flux	MW/m^2	6.7	5.2	6.8	7.3	7.6

mode, we believe FDF can accumulate a fluence over 10 years in the range 3-6 MW-yr/m^2. Because of the lower toroidal field, the power consumption in the facility drops from 500 to 348 MW, a substantial reduction in electric power costs. To maintain the confinement constraint on H-ITER98y2 = 1.6, the plasma current had to be kept up at 6.4 MA and the bootstrap fraction had to be lowered to 56%, an easily achieved value. The q then drops to 3.7, still an easily operable value. The fusion power is of course cut in half from 290 to 145 MW and the plasma energy gain Q drops to 3.5. The normalized beta is still 3.7. The peak divertor heat flux drops to 5.2 MW-m^{-2}.

Another such reduced performance mode that still preserves neutron wall loading 1.0 MW/m^2 is shown in the column labeled "Lower β_N fbs, H98" and is constructed assuming full field operation but more conservative β_N = 2.65, bootstrap fraction 54%, and lower confinement H98y2 = 1.36. Plasma current remains about the same but because of the lower bootstrap fraction the current drive power and so the total facility power goes up somewhat. Other such cases can be constructed because there is a wide operating space that preserves the nuclear science mission at neutron wall loading 1.0 Mw/m^2.

Higher Performance Modes that Reach for ARIES-AT Parameters

The desire for a DT facility that could carry Advanced Tokamak research beyond what ITER could do all the way to the kind of parameters characteristic of ARIES-AT was expressed by the magnetic fusion community through ReNeW, a planning activity of the Office of Fusion Energy Sciences [34]. To simplify, thrust 8 called for the ability to study/develop highly self-organized plasmas defined by simultaneous high energy gain (around 20) and high bootstrap current fractions (around 90%) on at least the several current diffusion time-scale or possibly in true steady-state but with no need or desire for a high fluence operation of such modes. Hence a pulsed, low duty factor operation, say less than 1000 s, perhaps just 100 s, might suffice. ARIES-AT parameters are operation at 90% of the beta limit, 90% bootstrap fraction, and energy gain around 20.

We feel that the essential mission of the FDF should focus on Fusion Nuclear Science and that that mission can be met with steady-state modest Q plasmas with much more conservative physics than anything like ARIES-AT. And that the combination of what will be learned at high Q with few thousand second pulses in ITER with the lower Q but true steady-state experience from the FDF will be an adequate basis to move to a high performance DEMO of the ARIES-AT type.

However it is a reasonable question to ask what technical reach might be embodied in the FDF that would allow that device to reach for ARIES-AT type parameters. We present such operating modes in the rightmost two columns of Table VII. The column labeled Advanced starts down the path to higher Q. With respect to the nominal baseline operation, the normalized β_N is turned up to 80% of the beta limit and the bootstrap fraction to 85%. Plasma current has risen to 7.09 MA but should be engineerable. The confinement quality

constraint is maintained at H98y2 = 1.6. The fusion Q rises to 12.4, the fusion power to 476 MW, and the neutron wall loading to 3.28 MW/m^2.

The column labeled Very Advanced takes the operation up to ARIES-AT parameters, 90% of the beta limit and 90% bootstrap fraction, again maintaining the same confinement constraint as the baseline. All these scenarios are done within the toroidal field and TF stress capabilities of the machine. Plasma current is up to 7.43 MA but probably still operable. The fusion Q rises to 20 under these circumstances with 634 MW fusion power output and neutron wall loading of 4.4 MW/m^2. This wall loading is high but under the ARIES-AT number of about 5 MW/m^2.

Our conclusion is that the FNSF-AT (FDF) has the potential for eventually operating Q about 20 with 90% bootstrap fractions at 90% of the beta limit, thus addressing the need to understand the highly integrated dynamics of dominantly self-heated and self-sustained burning plasmas. Such very advanced operation must be regarded as a long term, near final goal of the FDF research program, with no promises made as to the outcome of trying to achieve such parameters. Such operation would be of low duty factor in pulses less than 1000 s and so not be useful for the Fusion Nuclear Science studies that require fluence. But the low duty factor operation could allow some compromises in the blankets toward high neutron power flux handling at the expense of shielding. The one technical issue that emerged is the peak neutron wall loading at the midplane. For the FDF operating at $Q \sim 20$, bootstrap fraction 90% and 90% of the beta limit (the rightmost column in the table), the peak neutron wall loading gets up to about 4.4 MW/m^2. This is well beyond the nominal value operating value of 2 MW/m^2, but not beyond the needs of ARIES-AT (about 5 MW/m^2). This value may actually be achievable and operable in steady-state in FDF, especially considering it will come at the end of the blanket development program. The simultaneous achievement of the ARIES-AT physics parameters and the ARIES-AT neutron wall loading late in the FDF Program would be a major accomplishment enabling an ARIES-AT type DEMO.

III.B. SPHERICAL TORUS COMPONENT TEST FACILITY (ST-CTF)

Here we discuss only the main differences in how the ST-CTF design sheet is constructed as opposed to the FDF sheet. Single-turn TF centerposts are envisioned (with no insulators). There is no OH solenoid. Only a 10 cm inboard shield is provided; there is no inboard breeding blanket. An 80 cm outboard breeding blanket/shield is provided. At each aspect ratio the optimizer was allowed to vary the radial build of the TF coil and the current density in it, the central ion temperature, and the fraction of the TF coil that is copper in order to achieve a cooling water temperature rise in the TF coil less than 100°C, a peak neutron wall loading at the outer midplane of 2 MW/m^2, confinement quality H98y2 less than 1.6, density ratio to the Greenwald limit less than 0.8, and TF coil stress less than 276 MPa (40 ksi). The cost function minimized is the same as for the FDF case, which equally emphasizes small

machine size and small facility total power consumption. All machines are of course true steady-state with 100% non-inductive current drive. Results of the scan versus aspect ratio are given in the black (ST-CTF-Cu) curves in Figs. 3–11. In Fig. 3, one can see the minimum sized machine is at aspect ratio 1.7. However the minimum is very broad. Total facility power is 382 MW. We describe in detail below the calculations done by the spreadsheet for this ST-CTF baseline case, taking it as typical of all the varied aspect ratio cases the optimizer considers.

III.B.1. ST-CTF Baseline Geometry

Given the aspect ratio of 1.7, the elongation of 2.98 was obtained as 95% of the maximum stable elongation. An inner shield thickness of 0.1 m and an outer blanket/shield thickness of 0.8 m were assumed. The inner plasma gap was taken as 5 cm and the outer gap 8 cm.

The radial build of the TF coil selected by the optimizer is 0.240 m from the axis of symmetry of the machine and 0.02 m space is allocated to take the place of the non-existent OH solenoid. Given these values, the major radius and the minor radius of the baseline case are determined to be $R_0 = 1.04$ m and $a = 0.61$ m. The current density in the toroidal coil of 59.9 MA-m^{-2} is determined by the optimizer to give a peak neutron wall loading at the outboard midplane of 2 MW-m^{-2}. The toroidal field resulting from the determined TF geometry and the TF current density is 2.77 T. The TF stresses and cooling parameters then follow as in the formulae in the Toroidal Coil section above and set by the optimizer as constraints.

III.B.2. ST-CTF Baseline Plasma Parameters

The limiting value of β_N was 5.19 at 67% of the limiting β_N value, the same position with respect to the beta limit as in FDF.

A fixed bootstrap fraction of 75% was selected and used in all cases. Then the poloidal beta of 1.30 is calculated as above from the aspect ratio and the bootstrap fraction. Then the toroidal beta $\beta_T = 25.6\%$. The plasma current is 8.37 MA and the ITER value of q_{95} is 8.2.

An ion temperature of 10.7 keV was found by the optimizer. The helium fraction was 2%. The resulting central density is 5.4 x 10^{20} m^{-3} and the average density is 51% of the Greenwald density limit. The density profile was taken $S_N = 0.5$. The temperature profile was assumed more peaked $S_T = 0.75$.

The density at the top of the H-mode pedestal is 1.5 x 10^{20} m^{-3} and the pedestal temperature is 3.3 keV. The predicted offset counter rotation from non-resonant error fields is 21.3 krad/s which is 1.1% of the Alfven rotation indicating this should be sufficient rotation for resistive wall mode stabilization.

III.B.3. ST-CTF Baseline Auxiliary Heating and Current Drive

We took the required current drive power as 60% of the LHCD value plus 40% of the NBCD value, since ECCD has some problems of applicability. To drive the remaining 25% of the plasma current, 42 MW is required. The ST class of machines has some special challenges for auxiliary heating. The lower pedestal density and temperature, compared to FDF, should make the application of LHCD easier. However for EC, the EC fundamental frequency is 77.6 GHz and the second harmonic is 155 GHz. The cutoff density for fundamental outside launch O-mode is 0.75 x 10^{20} m^{-3}, so simple first harmonic outside launch O-mode cannot be used. The cutoff density for second harmonic O-mode is 2.98 x 10^{20} m^{-3} so perhaps this scheme could be used to heat and drive current well outside the half radius. For inside launch fundamental X-mode the cutoff density is 1.49 x 10^{20} m^{-3}, too low. Neutral beams have to be employed instead of EC. The required NBCD is slightly less than for ECCD. Positive ion NBI will not penetrate very far. Negative NBI may have to be used, a cost and complication we seek to avoid in the FDF.

III.B.4. ST-CTF Baseline Fusion Power

The baseline case has a fusion power of 111 MW. The plasma energy gain Q is 2.6. The peak neutron wall loading at the outer midplane is 2 MW/m^2, by design.

III.B.5. ST-CTF Baseline Toroidal Coil

Just as in FDF a peak hoop stress of 276 MPa is a constraint. Unlike FDF, the temperature rise in the cooling water is calculated to be large. It is small at high aspect ratio and rises as aspect ratio falls to 100°C at $A = 1.4$; it is 58°C in the baseline $A = 1.7$ case.

The overall height of the TF centerpost is 7.09 m.

The radial wedge sections are taken as 0.75 m in vertical height at the centerpost and 1.48 m at the return legs where they match onto half the toroidal circumference at the return legs. The radial thickness of the outer vertical return legs is determined by assuming a low 4 MA/m^2 current density in them. That thickness is 0.38 m.

The mass and power dissipation in the centerpost, the radial wedges, and the vertical return legs is given in Table VIII. Total TF power is 192 MW.

Table VIII
TF Coil Parameters for ST-CTF

	Mass (1000 kg)	Power Dissipated (MW)
Centerpost	11	176
Radial Wedges	506	4.3
Return Legs	342	11.7

III.B.6. ST-CTF Baseline OH Solenoid

There is no OH solenoid. The ST option requires startup without an OH transformer. This is one of the key feasibility issues for the ST option which must be proven out in experiments.

III.B.7. ST-CTF Baseline PF Coils

In Table IX, we give the radius, the area, the mass, and the power dissipated in the up-down symmetric pairs of PF coils. Clearly, since PF2 is so much larger than PF1, further optimization of the outer PF system can be made after another round of equilibrium calculations. However, our purpose here is just to get an approximate value of the power contribution of the PF coils to the total facility power.

Table IX
PF Coil Parameters

	Radius (m)	Area (m^2)	Mass (1000 kg) (1 of 2)	Power (MW) (1 of 2)
PF1	0.662	0.556	21	7.5
PF2	2.539	0.854	122	9.7
PF3	2.743	0.167	26	2.8

III.B.8. ST-CTF Baseline Energy Confinement Times

The required energy confinement time is 0.40 s. The same H-factor with respect to ITER's H-mode scaling, ITER98y2 of 1.6 was used as a constraint. Justification for this value would have to come from the ST databases. The H-factor against Petty's scaling is 1.71. The H-factor against ITER's L-mode scaling ITER89P is 3.38.

III.B.9. ST-CTF Baseline Divertor Heat Fluxes

The various parameters characterizing heat fluxes to the divertor were calculated using the methods described in Section II.H. The magnetic field of 2.8 T, safety factor of 8.2, and total heating power of 64 MW give a λ_q = 0.012 m from Loarte's formula. Two divertors with flux expansion 4 and 10 deg plate tilt were assumed. The power into the SOL was 28 MW. The raw P/R value is high, 62 MW/m. The anticipated peak heat flux on the outer divertor plate is just 6.8 MW-m^{-2}. Peak heat flux to the inner divertor is 1.1 MW/m^2. These values neglect completely radiation in the SOL and divertor, which should reduce the peak heat flux a factor of 2-4. Generally, because the ST machines are small and the heating power remains high, peak heat flux to the divertor is considered the second major feasibility issue for the ST approach. We have found a reasonable peak heat flux but the use of Loarte's scaling for the ST is suspect, since that scaling produces larger λ_q for smaller B field, larger

heating power, and larger q_{95}, all of which occur in the ST. But the scaling was derived only from data from the normal aspect ratio machines ASDEX Upgrade, DIII-D, and JET.

III.B.10. Comparison to ORNL ST-CTF and Potential for High Q Operation

In Table X, we give in the first column the key parameters of the ST-CTF that we derived above. Of course, Martin Peng and his co-workers at ORNL have for some time been advocating an ST-CTF [8,9]. They have taken the view of positioning their ST-CTF nominal operation without use of any advanced physics performance. For example they assume β_N about 3.5, which we would expect would be just 45% of the beta limit and is in fact below the no-wall beta limit. They also take a lower bootstrap fraction, 50%, and a more conservative confinement assumption H98y2 = 1.25. They take the same high elongation of 2.98 that we have taken and an ion temperature of 13.8 keV. When we put their very conservative physics assumptions in our ST spreadsheet, the optimizer reproduces very closely the nominal operating mode of the ST-CTF being advocated by Martin Peng and co-workers. We get an optimum ST-CTF at aspect ratio 1.7 with R = 1.32 m, which is almost identical to the ORNL baseline machine. The parameters of this baseline case are given in the column labeled ST-ORNL 2 MW/m^2. The fusion power is 177 MW and the peak neutron wall loading at the outer midplane is 2 MW/m^2. The fusion power calculated by ORNL is somewhat different since they calculate beam-target fusion reactions and we do not. Current drive power is 62 MW, the same as ORNL, but we are considering 60% LHCD and 40% NBCD and they consider NBCD. But the toroidal field, plasma current, density, and other parameters are almost identical to what ORNL have published as their baseline. This agreement provides confirmation of both the ORNL ST-CTF baseline and also our computational methods of assessing STs.

We went on to assess what sort of advanced tokamak performance ORNL's larger ST-CTF might have. This was done partially because of the interest expressed in thrust 8 of ReNeW in pathways to study high Q operation in true steady-state. The column labeled FDF Physics uses the physics assumptions we made for FDF but applied to the larger machine, meaning 67% of the beta limit giving β_N = 5.19 at A = 1.7 and κ 2.98, bootstrap fraction 75%, and H98y2 = 1.6, and T_i = 16 keV. For that case we would expect Q = 7.7 and peak neutron wall loading at the midplane of 4.15 MW/m^2. We do not know whether the ST database or first principles GLF23 calculations can support H98y2 = 1.6 in the ST.

To move toward higher gain capability, in the column labeled Advanced we turned β_N up to 80% of the beta limit and bootstrap fraction up to 85%, still with H98y2 = 1.6, and T_i = 15.3. Then Q becomes 12.1 and neutron power at the blanket 6.20 MW/m^2.

Table X
ST-CTF Operating Modes

	Summary		ST-CTF Optimum	ST-ORNL 2 MW/m^2	ST-ORNL FDF Physics	ST-ORNL Advanced	ST-ORNL Very Advanced	ST-ORNL Lower BT
A	Aspect ratio		1.7	1.7	1.7	1.7	1.7	1.7
a	Plasma minor radius	m	0.61	0.78	0.78	0.78	0.78	0.78
R_0	Plasma major radius	m	1.04	1.32	1.32	1.32	1.32	1.32
k	Plasma elongation		2.98	2.98	2.98	2.98	2.98	2.98
J_c	Centerpost current density	MA/m^2	59.9	42.7	42.7	42.7	42.7	40.0
P_f	Fusion power	MW	111	177	368	557	797	621
$P_{internal}$	Power to run plant	MW	355	475	442	450	452	414
Q_{plasma}	P_{fusion}/p_{aux}		2.6	2.9	7.7	12.1	19.6	14.8
P_n/A_{wall}	Neutron power at blanket	MW/m^2	2.0	2.0	4.2	6.3	9.0	7.0
β_T	Toroidal beta		0.26	0.17	0.26	0.32	0.38	0.38
β_N	Normalized beta	mT/MA	5.19	3.49	5.19	6.20	6.98	6.98
f_{bs}	Bootstrap fraction		0.75	0.50	0.75	0.85	0.90	0.90
P_{cd}	Current drive power	MW	42	62	47	46	41	42
I_p	Plasma current	MA	8.4	12.0	11.9	12.5	13.3	12.4
B_0	Field on axis	T	2.77	3.11	3.11	3.11	3.11	2.91
TF Stress	Stress in TF coil	MPA	276	276	276	276	276	242
q	Safety factor		8.2	8.2	8.2	7.8	7.3	7.3
$T_i(0)$	Ion temperature	keV	10.7	13.8	16.0	15.3	15.5	13.6
$n(0)$	Electron density	E20/m^3	5.4	3.6	4.6	6.1	7.2	7.2
$\bar{n}/n_{GR}$	Ratio to Greenwald limit		0.51	0.38	0.49	0.62	0.69	0.73
Z_{eff}			1.94	1.96	2.00	2.02	2.02	2.00
W	Stored energy in plasma	MJ	25	44	65	81	97	85
P_{AUX}	Total auxiliary power	MW	42	62	47	46	41	42
τ_E	τ_E	sec	0.4	0.45	0.53	0.52	0.49	0.51
HITER98 Y2	H factor over ELMY H		1.60	1.25	1.59	1.60	1.58	1.59
P_{SOL}/A_{div}	Peak divertor heat flux	MW/m^2	6.8	8.4	8.7	9.3	10.5	8.4

In the column labeled Very Advanced, we went to 90% of the beta limit and 90% bootstrap fraction, with still the same confinement constraint. T_i = 15.5 keV. The fusion Q rises to 19.6. But neutron wall loading is now 9 MW/m^2! These operating modes at high Q would likely be pulsed modes with very small duty factor and fluence. But still 9 MW/m^2 is a very high value, about twice reactor projections for peak wall loading. Peak divertor heat flux also gets rather high.

To try to lower the neutron wall loading, we made the column labeled Lower BT where we lowered the toroidal field to 2.91 T and adjusted T_i downward to 13.6 keV. But then Q then drops to 14.78 and neutron wall loading 6.98 MW/m^2.

We conclude here that the ST-CTF being advocated by ORNL may have advanced performance capability extending up to perhaps Q of 12, but whether such capability could be used will depend on whether their ST-CTF design embraces such AT elements (as we have embraced in FDF) as resistive wall mode (RWM) coils to enable operation in the wall stabilized regime and Resonant Magnetic Perturbation coils to eliminate ELMs.

III.C. INTER-MACHINE DISCUSSION AND ASPECT RATIO OPTIMIZATIONS

In Fig. 3, we see that the size of the FDF machines are about 2–3 times the size of ST-CTF machines. In Fig. 4, the fusion power rises rapidly for FDF as A is decreased while it is about constant versus A for ST-CTF machines.

The ST-CTF offers a machine about a factor of 3 smaller in size and probably in cost also. However, see the mission discussion in Section IV. The fusion power in the ST-CTF is small, 111 MW. The cases for ST-CTF with A above 2 are not really feasible machines since so many neutrons would be lost to the centerpost that TBR > 1 could not even be closely approached. Hence the ST with no inboard breeding or significant shielding and no OH solenoid is a really distinct machine branch, lying between aspect ratio 1.4 and 1.8 in practical terms and offering a very small nuclear science machine option.

The aspect ratio dependence of the power to run the plant is given in Fig. 4. The optimum FDF machine at A = 3.5 was chosen because the power to run the plant first gets down to 500 MW at that value of A. The power to run FDF and ST-CTF are rather similar, 500 MW and 400 MW, respectively.

The fusion power produced is given in Fig. 5. The nominal fusion power in FDF is 290 MW. For the ST-CTF it is 111 MW.

The current drive power is given in Fig. 6. The values at optimum for FDF and ST-CTF are quite close. FDF uses a combination of ECCD at about the half radius and LHCD out around r/a 0.8 to 0.9. The ST-CTF is envisioned to use LHCD and Negative Ion NBCD.

Figure 7 shows the common aspect ratio dependence of the β_N values used for the two machine types. In both cases the same 67% of the beta limit was used so that all machines at

the same A have the same proximity to the limit of stable operation. This is one important aspect of being able to compare two different types of machines with varying aspect ratio but with the same proximity to the limit of stable operation.

Similarly Fig. 8 shows the common 95% proximity to the elongation limit used for all these machines. For copper machines, their jointed TF coils allow PF coils inside the TF and close enough to the plasma to stabilize such high elongations, close to the ideal limit.

The closely similar values of toroidal beta are shown in Fig. 9.

Central densities are shown in Fig. 10 and the fact that all these machines in practical ranges stay below the Greenwald density limit is shown in Fig. 11. Central temperatures (one of the optimizer's free parameters) are shown in Fig. 12. Toroidal fields and plasma currents are shown in Figs. 13 and 14, respectively.

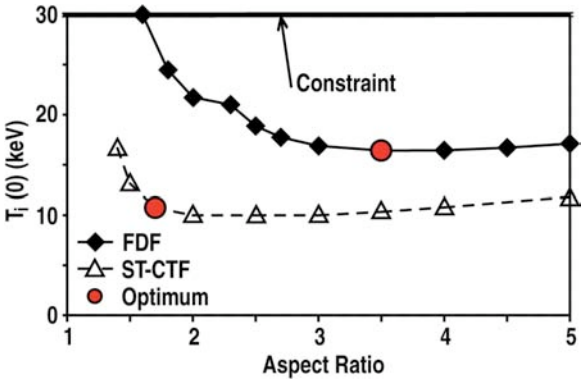

Fig. 12. Central ion temperatures versus A.

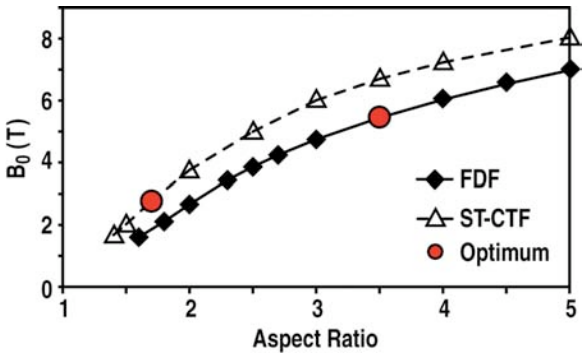

Fig. 13. Toroidal field versus A.

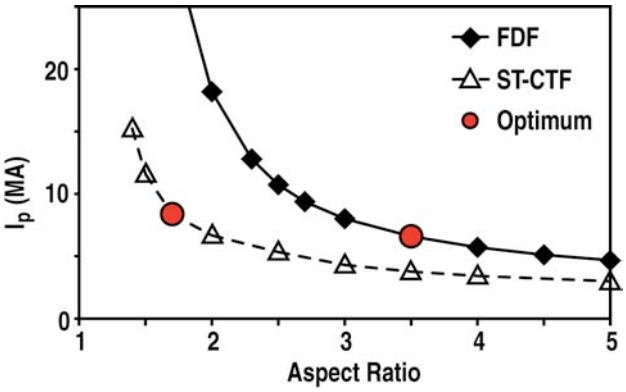

Fig. 14. Plasma current versus A.

The gross required values of τ_E are shown in Fig. 15. The ST-CTF has a much lower value than FDF. These confinement times are shown as H-factors with respect to ITER98y2 scaling in Fig. 16 and ITER89P scaling in Fig. 17. The value H98y2 < 1.6 was in general

used as a constraint. All the ST-CTF machines are at the constraint value. FDF machines have lowering confinement requirement below $A = 2.3$.

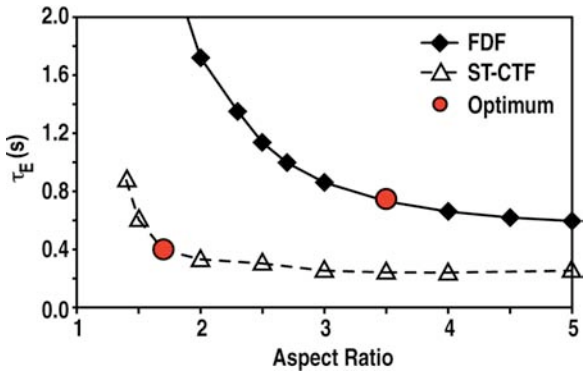

Fig. 15. Energy confinement time versus A.

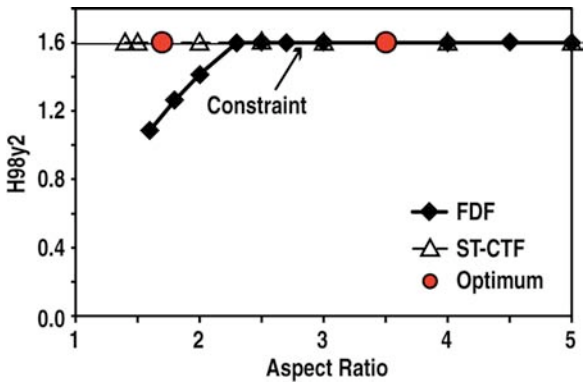

Fig. 16. Confinement multiplier times ITER H-mode scaling.

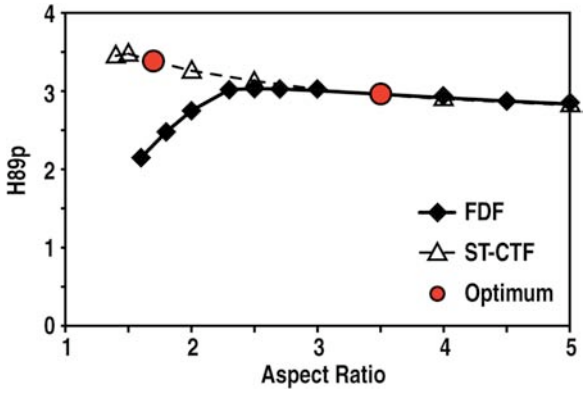

Fig. 17. Confinement multiplier times ITER L-mode scaling.

IV. DISCUSSION AND CONCLUSIONS

In the sections above, we have given a comprehensive exposition of the methods by which we have assessed two candidates for a Fusion Nuclear Science Facility for the U.S. fusion program and we have described those machine options in detail. Those machines are aimed at providing research devices to enable development of fusion's energy applications and the operating modes needed in DEMO. Those devices would be used to learn how to close the fusion fuel cycle and make electricity and hydrogen from the fusion process in order to assure net tritium production for the DEMO to follow. They are generically called the Fusion Nuclear Science Facility (FNSF). Two reasonable candidates for those purposes have been described, a normal aspect ratio tokamak called the Fusion Development Facility (FDF) sometimes the FNSF-Advanced Tokamak and the Spherical Torus-Component Test Facility (ST-CTF) sometimes called the FNSF-ST.

To give any kind of assessment of the relative merits of the two machine approaches, we must look at how their ability to carry out the research is affected by the type of machine being envisioned.

The essential design feature of FDF and ST-CTF that allows them to be effective research machines, enabling frequent planned changeouts and maintenance of the blanket structures inside the TF coil is their jointed copper TF coil. The TF coil joint allows a vertical maintenance scheme in which the blanket structures inside the TF coil can be built as axisymmetric rings structures and maintained and changed out quickly as large units. This vertical maintenance approach is shown in Fig. 18. Furthermore their construction as axisymmetric rings allows the kind of precision toroidal alignment of plasma facing surfaces necessary to handle the power outflows from the plasma.

A candidate research plan for the FDF is shown in Fig. 19 and is probably typical of the program that would be undertaken on ST-CTF. It exhibits clearly the plan to make three major changeouts of the full blanket structures, not to mention necessary similar maintenance operations. An initial 4 year commissioning period is envisioned in which the working fuel will progress from H to D to DT. Fusion power will rise during those years to 150 MW in 10 minute pulses. The basic operating modes of the machine can be developed in this phase without dependence on the fusion power since the installed auxiliary power will be sufficient. A helium-cooled solid breeder blanket will be installed from the start and the TBR will gradually be improved from about 0.9 to ~1.1 by the end of the First Main Blanket phase as the device operators learn better how to operate the blanket systems and the entire closed loop tritium system. Until this first main blanket starts to produce net tritium, the facility will be a net tritium consumer with a need for about 1 kg of external supply, later to be returned. By the end of this first main blanket phase, true steady-state operation will have been developed with duty factor 0.2 and fusion power 250 MW and wall loading 2 MW/m^2. Net tritium produced will be 0.56 kg per year. Two ports will be devoted to a test blanket module

program as on ITER. It is envisioned that teams of universities, laboratories, and industry will propose to field and study test blanket modules on FNSF as a user facility. In the port blanket sites, the first two TBMs will have been tested.

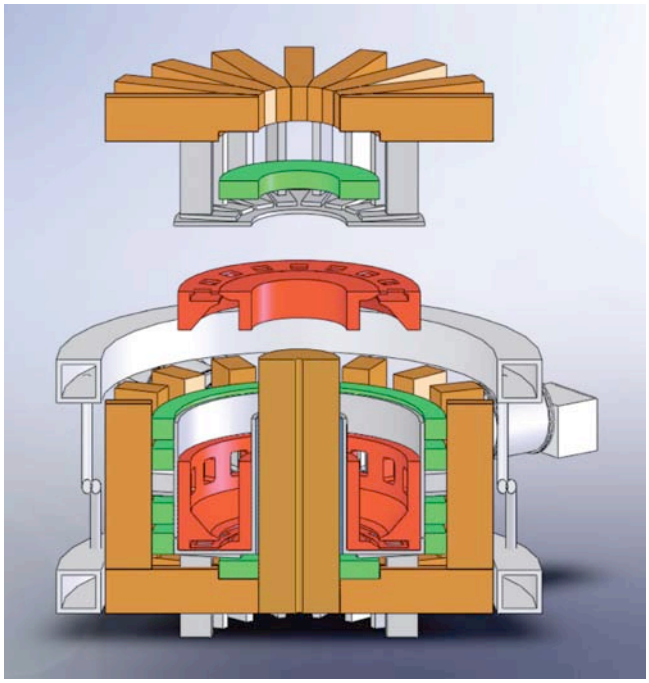

Fig. 18. FDF baseline maintenance scheme allows crane lift of toroidally continuous ring structures, assuring strength of blankets and precision toroidal alignment of the divertor surface. Red structures are the full blanket assemblies.

Year	1	2	3	4	5	6	7	8	9	10	11	12	13	14	15	16	17	18	19	20	21	22	23
	← START UP → H D DT				FIRST MAIN BLANKET							SECOND MAIN BLANKET							THIRD MAIN BLANKET				
Fusion Power (MW)	0	0	125		125			250				250			250				250			400	
P_N/A_{WALL} (MW/m^2)			1		1			2				2			2				2			3.2	
Pulse Length (Min)	1		10		SS			SS				SS			SS				SS			SS	
Duty Factor	0.01		0.04		0.1			0.2				0.2			0.3				0.3			0.3	
T Burned/Year (kg)			0.28		0.7			0.8				2.8			4.2				4.2			5	
Net Produced/Year (kg)					−0.14			0.56				0.56			0.84				0.84			1	
Main Blanket	He Cooled Solid Breeder Ferritic Steel											Dual Coolant Pb-Li Ferritic Steel							Best of TBMs RAFS?				
TBR					0.8			1.2				1.2			1.2				1.2			1.2	
Test Blankets						1,2						3,4		5,6					7,8		9,10		
Accumulated Fluence (MW-yr/m^2)			0.06					1.2							3.7							7.6	

Fig. 19. Operational and blanket development schedule of FDF. Duty factor is the fraction of a year the device is on and making plasma and fusion power.

A 2-year shutdown will enable changing to the second main blanket phase. This blanket is envisioned to be the dual coolant lead-lithium blanket. By the end of this phase, the duty factor will be 0.3 and the tritium produced per year 0.84 kg. TBMs 3, 4, 5, and 6 will have been tested. Accumulated fluence on anything that has remained in the machine all 16 years will be 3.7 MW-yrs/m^2.

Then there will be a 2 year shutdown to change to the third main blanket phase. The third main blanket will be built from the best result of the first two TBMs. At the end of this phase, the machine will reach for its very advanced operating modes, perhaps with fusion power reaching 400 MW and wall loading 3.2 MW/m^2. Net tritium production per year will reach 1 kg. TBMs 7, 8, 9, and 10 will have been tested. Accumulated fluence for the machine lifetime to date will reach 7.6 MW-yrs/m^2.

The price paid for this flexibility in FDF or ST-CTF is the high power consumption in the copper coils and, in the case of the FDF, a size twice that of the ST-CTF to accommodate sufficiently massive TF coils to keep the power consumption in a reasonable range.

The main advantages of the FDF is that it is deliberately configured to essentially be ready to move to construction now and that it clearly has the potential to develop the advanced operating modes needed for DEMO. It's construction features are all based on the existing tokamaks DIII-D and Alcator C-mod. It is a rather prosaic copper coil tokamak. Its physics basis for its nominal operations is either in hand or can be thoroughly in hand in the next few years, with proper focus in the U.S. research program.

The main advantages of the ST-CTF are that it also is a machine we are nearly ready to construct today and it is the smallest and lowest cost (by about a factor two) next step machine being considered. The version suggested by ORNL is also positioned to use only very conventional, already in-hand physics. The main drawbacks are that it requires experimental demonstration of an effective method of startup without an OH transformer coil, high peak divertor heat flux arising from its small size, and the advocated machine may not have Advanced Tokamak reach. It appears to us that the transformerless startup issue can be settled in the next few years. Our analysis in this paper suggests the peak heat flux problem may not be as severe as generally thought and we suggest pathways to AT operation that may be available in the ST-CTF as constructed.

REFERENCES

[1] "Priorities, Gaps and Opportunities: Towards a Long-Range Strategic Plan for Magnetic Fusion Energy" (FESAC, October, 2007), http://www.ofes.fusion.doe.gov/fesac.shtml.

[2] R. AYMAR, P. BARABASCHI and Y. SHIMOMURA, Plasma Phys. Control. Fusion **44**, 519 (2002).

[3] R. D. STAMBAUGH et al., "Research Thrusts Made Possible by a Fusion Development Facility," General Atomics White Paper WP 09-01 (2009); http://burningplasma.org/web/ReNeW/whitepapers/1-01%20FDF_ReNeW_Brief_Final.PDF

[4] A. M. GAROFALO et al., IEEE Trans. Plasma Sci. **38**, 461 (2010).

[5] V. S. CHAN et al., Fusion Sci. Technol. **57**, 66 (2010).

[6] F. NAJMABADI et al., Fusion Eng. Design **80**, 3 (2006).

[7] MOHAMED A. ABDOU et al., Fusion Sci. Technol. **29**, 1 (1996).

[8] Y-K. M. PENG et al., Plasma Phys. Control. Fusion **47,** B263–B283 (2005).

[9] Y. K. M. PENG et al., Fusion Sci. Technol. **56**, 957 (2009).

[10] A. LOARTE et al., Nucl. Fusion **47,** S203–S263 (2007).

[11] R. D. STAMBAUGH, L. L. LAO and E. A. LAZARUS, Nucl. Fusion **32**, 1642 (1992).

[12] E. A. LAZARUS, J. B. LISTER and G. G. NEILSON, Nucl. Fusion **30** (1990) 111.

[13] Y. R. LIN-LIU and R. D. STAMBAUGH, Nucl. Fusion **44**, 548 (2004).

[14] P. B. SNYDER et al., Nucl. Fusion **44**, 320 (2004).

[15] P. B. SNYDER et al., Phys. Plasmas **9**, 2037 (2002).

[16] P. B. SNYDER et al., Nucl. Fusion **47**, 961 (2007).

[17] P. B. SNYDER and H. R. WILSON, Plasma Phys. Control. Fusion **45**, 1671 (2003).

[18] A. M. GAROFALO et al., Phys. Rev. Lett. **101**, 195005 (2008).

[19] A. J. COLE et al., Phys. Rev. Lett. **99**, 065001 (2007).

[20] R. D. STAMBAUGH, "Review of ITER Physics Issues and Possible Approaches to their Solution," Proc. 21st IAEA Fusion Energy Conference, Chengdu, China, 2006; http://www-pub.iaea.org/MTCD/Meetings/FEC2006/it_1-2.pdf

[21] G. TONON, "Current Drive Efficiency Requirements for an Attractive Steady-State Reactor," Proc. Workshop Tokamak Concept Improvement, Varenna, Italy, August 1994, p. 233.

[22] R. H. FOWLER, J. A. HOLMES and J. A. ROME, "NFREYA – A Monte Carlo Beam Deposition Code for Noncircular Tokamak Plasmas," Oak Ridge National Report ORNL/TM-6845 (1969).

[23] A. H. KRITZ et al., Proc. 3rd International Symposium on Heating in Toroidal Plasmas, Grenoble, Italy, 1982 (ECE, Brussels, 1982), Vol. 2, p. 707; Y. R. LIN-LIU, V. S. CHAN, and R. PRATER, Phys. Plasmas **10**, 4064 (2003).

[24] A. P. SMIRNOV, R. W. HARVEY and K. KUPFER, Bull Am. Phys. Soc. **39**, 1626 (1994).

[25] H. S. BOSCH and G. M. HALE, Nucl. Fusion **32**, 611 (1992).

[26] C. C. Petty et al., Fusion Sci. Technol. **43**, 1 (2003).

[27] ITER Physics Basis Editors, ITER Physics Expert Group Chairs and Co-Chairs, and ITER Joint Central Team and Physics Integration Unit, "ITER Physics Basis 1999," Nucl. Fusion **39**, 2137 (1999).

[28] M. MURAKAMI et al., Phys. Plasmas **13**, 056106 (2006).

[29] A. M. GAROFALO et al., Phys. Plasmas **13**, 056110 (2006).

[30] J. R. FERRON et al. "Development in DIII-D of High Beta Discharges Appropriate for Steady-State Tokamak Operation with Burning Plasmas," Proc. 22nd IAEA Fusion Energy Conference, Geneva, Switzerland, 2008; http://www-pub.iaea.org/MTCD/Meetings/FEC2008/ex_p4-27.pdf

[31] A. FASOLI et al., Nucl. Fusion **49**, 104005 (2009).

[32] S. MALANG (private communication).

[33] C. P. C. WONG (private communication).

[34] "Research Needs for Magnetic Fusion Energy Sciences," Report of the Research Needs Workshop, Bethesda, Maryland 2009, edited by P. Weiser.

ACKNOWLEDGMENT

This work was supported in part by General Atomics internal funding and in part by the U.S. Department of Energy under DE-FG02-09ER54513.